Geophysical Journal International
March 2010, Volume 180 Issue 3, Pages 976 - 998
http://dx.doi.org/10.1111/j.1365-246X.2009.04477.x

The definitive version is available at http://www3.interscience.wiley.com/

Structure and rifting evolution of the northern Newfoundland Basin from Erable multichannel seismic reflection profiles across the southeastern margin of Flemish Cap

J. K. Welford[1, *], J. A. Smith[2], J. Hall[1], S. Deemer[1], S. P. Srivastava[3] and J.-C. Sibuet[4]

[1] Department of Earth Sciences, Memorial University of Newfoundland, St John's, NL, Canada. [2] BP Canada Energy Company, Calgary, AB, Canada
[3] Geological Survey of Canada, Bedford Institute of Oceanography, Dartmouth, NS, Canada
[4] Ifremer, Centre de Brest, Département des Géosciences Marines, Plouzané, France

*: Corresponding author : J. K. Welford, email address : kwelford@mun.ca

Abstract:

We present the results from processing and interpreting five lines from the 1992 Erable multichannel seismic reflection experiment extending from the southeastern margin of Flemish Cap into the northern Newfoundland Basin. These profiles reveal significant along strike variations in the rifting styles experienced by Flemish Cap. In the southwest, a 100-km-wide transition zone is identified between thinned continental crust and thin oceanic crust. Similar to the conjugate Galicia Bank and Iberian margins, this transition zone contains a section of deep basement adjacent to a series of shallower ridges and is interpreted as exhumed serpentinized mantle. Along strike towards the northeast, this transition zone pinches out completely within 100 km and is replaced by thin oceanic crust directly adjacent to thinned continental crust. By interpreting nearby seismic profiles and profiles on the conjugate margins using the same classification criteria, we construct regional maps of the distribution of crustal domains on both sides of the North Atlantic. These maps reveal significant variations in rifting style on the conjugate margins and along strike of each margin and also highlight the role of ancient transfer zones in compartmentalizing these rifting variations into four distinct regions. We propose that the limited localization of shallow topographically high serpentinized peridotite ridges on the Newfoundland-Iberia and Flemish Cap-Galicia Bank conjugate margins, was directly related to an increase in the rate of extension following the separation of Flemish Cap and Galicia Bank which exhumed deeper, less serpentinized mantle.

Keywords: Controlled source seismology • Submarine tectonics and volcanism • Continental margins: divergent • Continental tectonics: extensional • Crustal structure • Atlantic Ocean

1. Introduction

The non-volcanic/magma-poor Newfoundland/Iberia and Flemish Cap/Galicia Bank conjugate continental margins (Fig. 1) are ideal locations for studying the dynamics of rifting since most of their extensional crustal structures have not been altered or obscured by magmatic processes. Consequently, these margins have been the focus of significant geophysical investigation (Boillot et al., 1980; Boillot et al., 1987; Shipboard Scientific Party, 1987; Keen & de Voogd, 1988; Mauffret et al., 1989; Todd & Reid, 1989; Tucholke et al., 1989; Whitmarsh et al., 1990; Pinheiro et al., 1992; Beslier et al., 1993; Whitmarsh et al., 1993; Reid, 1994; Sibuet et al., 1995; Funck et al., 2003; Henning et al., 2004; Hopper et al., 2004; Hopper et al., 2006; Lau et al., 2006a; Lau et al., 2006b; Shillington et al., 2006; van Avendonk et al., 2006; Clark et al., 2007; Afilhado et al., 2008; Deemer et al., 2009). While early attention was focused on central Iberia and Galicia Bank, seismic data coverage over the Newfoundland and Flemish Cap margins has increased to the point that better comparisons and interpretations are now possible for the conjugate pair. Of key importance to studies of non-volcanic/magma-poor margins is the nature of the transitional zone that exists between continental and oceanic crust (Louden & Chian, 1999; Srivastava et al., 2000; Whitmarsh et al., 2001a; Russell & Whitmarsh, 2003). On the Iberian and Galicia Bank margins, the nature of the transition zone has been well constrained from seismic profiling accompanied by extensive drilling. In the Newfoundland Basin, an increasing number of seismic surveys have illuminated the transition zone but with only one drillhole available for ground truthing (Shipboard Scientific Party, 2004; M¨untener & Manatschal, 2006; Tucholke & Sibuet, 2007), significant debate remains regarding the nature of this transitional crust (Lau et al., 2006a; Lau et al., 2006b; Shillington et al., 2006; van Avendonk et al., 2006; van Avendonk et al., 2009; Deemer et al., 2009).

In 1992, the Erable project was undertaken jointly by the Geological Survey of Canada's Atlantic Geoscience Centre (AGC) and the Institut français de recherche pour l'exploitation de la mer (Ifremer). The project involved the acquisition of multiple 2-D multichannel seismic reflection profiles in the Newfoundland Basin and across the margins of Flemish Cap. The goal of this study is to present and provide interpretations for five of the profiles which extend across the southeastern margin of Flemish Cap into the deeper waters of the Newfoundland Basin, namely profiles E33, E36, E53, E54 and E56 (Fig. 2). Our profiles bridge between two of the lines from the more recent Study of Continental Rifting and Extension on the Eastern Canadian Shelf (SCREECH) project collected in 2000. The SCREECH profiles revealed very different structures (Funck et al., 2003; Hopper et al., 2004; Shillington et al., 2006; van Avendonk et al., 2006; Tucholke et al., 2007; Deemer et al., 2009), despite their close proximity, and the newly presented Erable profiles allow for a more detailed understanding of how the margin varies over a few hundred kilometers.

We combine the results from the Erable profiles with those of the SCREECH seismic profiles, two Ocean Drilling Program (ODP) drill sites and other geophysical data to place boundaries on continental, transitional and oceanic crust. In the absence of coincident velocity control along the Erable profiles, the placement of crustal domain boundaries is heavily influenced by velocity constraints from earlier seismic refraction studies in close proximity to the Erable lines (Todd & Reid, 1989; Funck et al., 2003; van Avendonk et al., 2006). The more comprehensive data coverage provided by the Erable data along the southeastern margin of Flemish Cap and into the northern Newfoundland Basin allows us to obtain valuable geometrical constraints on rifting. By comparing these constraints with those obtained along strike and on the Iberian and Galicia Bank margins, we investigate regional variations in rifting style and speculate about the timing of rifting, rifting processes and the influence of features like transfer zones on how these specific conjugate margins evolved.

2 TECTONIC SETTING OF THE NEWFOUNDLAND AND FLEMISH CAP MARGINS

The Grand Banks and Flemish Cap make up the continental shelf of the offshore Newfoundland margin and consist of basement rocks of the Avalon terrane. This terrane, which was originally part of the Gondwanan supercontinent, was accreted to the eastern margin of North America (Laurentia) during the closing of the Iapetus ocean in Paleozoic time during the Appalachian Orogeny (Haworth & Keen, 1979; Williams, 1984; Williams, 1995). Mesozoic opening of the modern North Atlantic ocean later occurred within this terrane. From paleoreconstructions of the margin in Aptian time (chron M0) at the inferred initiation of seafloor spreading (e.g., Srivastava and Verhoef (1992)), the conjugates for the Grand Banks margin, the southeastern margin of Flemish Cap and the northeastern margin of Flemish Cap were, respectively, the central Iberian margin, the Galicia Bank of the northern Iberian margin, and the Goban Spur, offshore Ireland.

Our study area focuses on the southeastern margin of Flemish Cap, a prominent sub-circular submarine knoll whose tectonic history remains a topic of active research (Srivastava & Verhoef, 1992; Enachescu, 2006; Sibuet et al., 2007b). At 30 km in thickness, this block of continental crust is located northeast of the Grand Banks and has been interpreted as an extension of the Avalon terrane due to its core of Hadrynian (Late Proterozoic) rocks (King et al., 1985; Enachescu, 1992). The flat-topped knoll lies under less than 200 m of water and is onlapped by a very thin cover of Mesozoic and Cenozoic sediments which are folded and faulted along the west to southwest edge of the cap but are relatively undisturbed elsewhere.

Prior to separation of Iberia and Eurasia from North America, an initial rifting episode during the Triassic started to create many of the half graben basins found on the Grand Banks (e.g., Carson-Bonnition, Jeanne d'Arc, Whale, Horseshoe) and on the Galicia Bank margin (e.g., Inner Galicia, Lusitanian; Murillas et al. (1990)) while the Flemish Cap was not affected until the early Jurassic (Sibuet et al., 2007b). From Late Jurassic to Early Cretaceous another phase of rifting progressed diachronously from south to north, leading to the east-west separation of the Grand Banks from central Iberia and then to the northwest-southeast separation of the southeastern margin of Flemish Cap from Galicia Bank (Williams, 1984; Tucholke et al., 1989; Grant & McAlpine, 1990). A final phase of separation of Flemish Cap from Galicia Bank occurred in the Late Cretaceous (de Graciansky & Poag, 1985; Tucholke et al., 1989; Hopper et al., 2006; Tucholke & Sibuet, 2007), separating the northeast margin of Flemish Cap from the Goban Spur, offshore Ireland.

Plate reconstructions of the North Atlantic margins prior to separation using large-scale plates corresponding to North America, Iberia and Europe have generally resulted in significant overlap between Flemish Cap and Galicia Bank, even when extension within the plates has been taken into account (Le Pichon et al., 1977; Srivastava & Verhoef, 1992). Consequently, it has been suggested that Flemish Cap and Galicia Bank acted as microplates during rifting, moving relative to their adjacent larger plates (Le Pichon et al., 1977; Srivastava & Verhoef, 1992; Srivastava et al., 2000; Sibuet et al., 2004). Sibuet et al. (2007b) generated a new paleoreconstruction using Bouguer gravity data to estimate the amount of extension experienced within the larger plates assuming the microplate model. They concluded that Flemish Cap originated in the region now occupied by the Orphan Basin, rotating out in a clockwise direction 43^o (relative to Iberia) during the Late Triassic to Early Cretaceous and moving 200-300 km southeastward (relative to North America) from Late Jurassic to early Aptian time (Srivastava & Verhoef, 1992; Srivastava et al., 2000; Enachescu, 2006; Sibuet et al., 2007b). With significant microplate reorganization postulated within the North American plate occurring over the same timescale as rifting and separation between North America, Iberia and Europe, the tectonic evolution of Flemish Cap and its margins is complex and along margin variability should be significant, as has been revealed by recent studies (Funck et al., 2003; Hopper et al., 2004; Shillington et al., 2006; van Avendonk et al., 2006).

3 PAST WORK ON THE GALICIA BANK AND IBERIAN MARGINS

3.1 Galicia Bank

Conjugate to the southeastern margin of Flemish Cap, the Galicia Bank, which makes up the northern section of the Iberian margin, is a shallow submarine plateau with a thin sedimentary cover that has been interpreted as a tilted Mesozoic continental fault block that was uplifted by early Cenozoic Pyrenean tectonics (Mougenot et al., 1984). Multichannel seismic reflection data were collected over the Galicia Bank margin by the Institut Français du Pétrole (IFP) in 1975 and

1980 (de Charpal et al., 1978; Montadert et al., 1979; Chenet et al., 1982). The key discovery from the seismic profiling was the presence of a prominent reflection, the S-reflector (Boillot & Winterer, 1988; Boillot et al., 1988), which is generally interpreted as a top to the west detachment fault that, from east to west, extends from the middle crust, into the lower crust, and then nears or reaches the crust-mantle boundary over a distance of 20 km (Reston, 1996; Reston et al., 1996; Whitmarsh et al., 1996).

Another key discovery from the Galicia Bank studies is the presence of a north-south trending ridge of serpentinized peridotites at the seafloor adjacent to thinned continental crust. These peridotites, confirmed through dredging (Boillot et al., 1980) and ODP drilling (Shipboard Scientific Party, 1987), were the first mantle rocks to be sampled from the ocean-continent transition zone (OCTZ) and served as the basis for theories of mantle exhumation occurring during the breakup process (Boillot et al., 1980; Shipboard Scientific Party, 1998). The serpentinized peridotites recovered from ODP Leg 103, Site 637, consist of subcontinental mantle rocks, exposed to the seafloor during the final stages of the rifting process (Evans & Girardeau, 1988; Girardeau et al., 1988; Kornprobst & Tabit, 1988; Sibuet et al., 1995).

Just seaward of the peridotite ridge, inferred oceanic crust is thin (2.5-3.5 km), gradually thickening to approximately 7 km (normal ocean crust; White (1992)) over a distance of approximately 20 km (Whitmarsh et al., 1996). This narrow zone of anomalously thin oceanic crust, interpreted to be underlain by serpentinized mantle (Sibuet et al., 1995; Whitmarsh et al., 1996), has been attributed to a limited magma supply due to the slow conductive cooling of the mantle during a long rifting stage (Bown & White, 1994; White et al., 1992).

3.2 Iberia Abyssal Plain

Conjugate to the Grand Banks section of the Newfoundland margin, the central Iberian margin consists of the Iberia Abyssal Plain which has been the focus of significant geophysical investigation. From extensive drilling during both the Deep Sea Drilling Program (DSDP) and the Ocean Drilling Program (ODP) (Shipboard Scientific Party, 1979; Pinheiro et al., 1996; Whitmarsh & Wallace, 2001), thinning of the continental crust of the Iberia Abyssal Plain south of Galicia Bank is interpreted to have been accommodated by both low angle detachment faults and high angle normal faults (Whitmarsh et al., 2000; Whitmarsh & Wallace, 2001). In contrast to the Galicia Bank to the north, these inferred faults, some of which have been imaged seismically (Krawczyk et al., 1996; Pickup et al., 1996), appear to sole at different depths within the mantle.

Adjacent to the rotated fault blocks of thinned continental crust is a 120 km wide bimodal transition zone. Landward, the transition zone is characterized by deep basement with low top-of-basement reflectivity consisting of a thin basement layer underlain by a 7.3-7.9 km/s velocity layer with a thickness of up to 4 km (Pickup et al., 1996; Dean et al., 2000). This part of the transitional zone has been interpreted as exhumed mantle that has been highly serpentinized through faulting and the influx of seawater (Pickup et al., 1996; Dean et al., 2000). At the seaward end of the transition zone, a 50 km wide section of shallow basement with arguably increased basement relief and reflectivity contains two peridotite ridges. These ridges are thought to be connected to those identified to the north along the Galicia Bank margin. Basement drilling within the transitional zone has revealed the presence of exhumed serpentinized peridotites (Whitmarsh & Wallace, 2001), representative of subcontinental mantle (Abe, 2001; Hébert et al., 2001). Seaward of the peridotite ridges, a two-layer velocity structure, typical for layer 2 and 3 of normal oceanic crust, is observed (Dean et al., 2000).

4 PAST WORK ON THE NEWFOUNDLAND AND FLEMISH CAP MARGINS

A total of 31 lines were collected in 1984 during the first large-scale deep multichannel seismic reflection program off the southeastern Newfoundland margin (some of which are labelled with NB in Fig. 2A) but with only a few line segments published (Tucholke et al. (1989); all processed sections are available for download from the Marine Seismic Data Center at the University of Texas at Austin (http://www.ig.utexas.edu/sdc)), the first crustal-scale images of the Newfoundland and Flemish Cap margins emerged from the Geological Survey of Canada's (GSC) Frontier Geoscience Project (FGP) from 1984 to 1990. These data were complemented by coincident seismic refraction/wide-angle reflection profiles collected by the GSC from 1983 to 1992. The main finding along the FGP profiles was the identification of a dominant landward dipping reflector interpreted as an abrupt continent-ocean boundary off the Grand Banks of the Newfoundland margin along F85-2 and off the northeastern margin of Flemish Cap along F85-3 (Fig. 2; Keen et al. (1987) and Keen and de Voogd (1988)). The latter interpretation along F85-3 was supported by seismic refraction results seaward of the boundary which were consistent with the presence of oceanic crust (Reid & Keen, 1990a). From subsequent seismic refraction surveying along line F85-2 (Reid, 1994), a narrow transition zone of anomalously thin oceanic crust underlain by serpentinized mantle was interpreted between continental and normal oceanic crust.

A seismic refraction survey collected by the GSC in 1985 along the southeastern margin of Flemish Cap (Todd & Reid, 1989) provides a key set of velocity constraints for the interpretation of the Erable profiles. Velocity-depth models from 6 ocean bottom seismometers (Fig. 2B) provide the only nearby velocity constraints for line E54 and for the landward extent of line E56. The simple velocity models, which are coarse with unspecified uncertainties, reproduce the main trends in the recorded data. From Todd and Reid (1989), three models (HU-9, HU-10, and HU-11) revealed velocity structures consistent with continental crust and three others (HU-1, HU-2, HU-18) were interpreted as oceanic crust based on the presence of a strong 7.3 km/s refracted arrival in the data, attributed to layer 3 oceanic crust. One anomalous model (HU-6) with a thin high gradient layer consistent with layer 2 oceanic crust immediately overlying typical unaltered mantle velocities was interpreted as an oceanic fracture zone (Todd & Reid, 1989). It has been suggested that the models from HU-1, HU-2 and HU-18 could equally represent thin layer 2 oceanic crust underlain by serpentinized mantle (Reid, 1994; Louden & Chian, 1999), an interpretation that is similar to what has been suggested for parts of the conjugate Galicia and Iberian margins (Whitmarsh et al., 1990; Pinheiro et al., 1992; Whitmarsh et al., 1993).

The recent SCREECH project in 2000 was a collaborative project between Woods Hole Oceanographic Institution, the University of Wyoming, the Danish Lithosphere Centre, Dalhousie University and Memorial University of Newfoundland. This project involved the acquisition of refraction/wide-angle seismic reflection, multichannel seismic reflection, magnetic, gravity and multi-beam bathymetric data along 3 major transects, SCR1, SCR2 and SCR3, over the continental shelf into the Newfoundland Basin (Fig. 2). An additional line, SCR104, which was acquired to tie lines SCR1 and SCR2, is also relevant to our study but has not been previously published. The SCREECH results have demonstrated the presence of transitional crust offshore Newfoundland with the lateral extent of transitional crust generally decreasing northeastward along the margin and disappearing along the southeastern edge of Flemish Cap (Funck et al., 2003; Hopper et al., 2004; Hopper et al., 2006; Lau et al., 2006a; Lau et al., 2006b; Shillington et al., 2006; van Avendonk et al., 2006; Deemer et al., 2009). Velocity constraints from profiles SCR1 (Funck et al., 2003) and SCR2 (van Avendonk et al., 2006) were key to the interpretation of crustal domains along Erable lines E33, E36 and the seaward portion of line E56. The velocity model for profile SCR1 (Funck et al., 2003) was obtained using a layer-stripping forward-modelling approach that modelled both refracted and reflected phases. Where the model resolution was poor, model velocities were constrained by analysis of the coincident multichannel data. For profile SCR2 (van Avendonk et al., 2006), reflected arrivals were not considered and a laterally smoothed model was obtained using a tomographic inversion of the refracted arrivals. Model resolution was best for features larger than 20 km by 8 km.

ODP drilling in the Newfoundland Basin has been limited to sites 1276 and 1277 (labelled 6 and 7 in Figs. 2A and 2B) from Leg 210 in 2003 (Shipboard Scientific Party, 2003; Tucholke & Sibuet, 2007). Site 1276 was drilled on presumed transitional crust and bottomed out in diabase sills that intruded Aptian to Albian sediments approximately 100-200 m above the anticipated depth of the top of basement. The upper sill corresponds with the U reflector, a high amplitude event that is widespread within the Newfoundland Basin (Tucholke et al., 1989; Shillington et al., 2007). Since basement was not penetrated at ODP Site 1276, a second drilling location, Site 1277, was chosen on a basement high in an area initially interpreted as oceanic crust (Shipboard Scientific Party, 2004; Shillington et al., 2004). Drilling into basement revealed gabbro and basalt fragments as well as serpentinized peridotites, interpreted as having acquired their geochemical signature pre-rift, possibly in relation to a subduction in the Caledonian, or an even older orogenic event (Müntener & Manatschal, 2006). The serpentinized peridotites recovered from Site 1277 are the only basement rocks to have been sampled from the transition zone in the Newfoundland Basin.

5 DATA ACQUISITION AND RESULTS

Data acquisition for the Erable project was undertaken aboard the Canadian research ship CSS Hudson. The ship was outfitted with multichannel seismic equipment belonging to Ifremer. An array of 8 Bolt air guns with a total capacity of 92 litres was fired every 38.8 seconds at a cruising speed of 5 knots corresponding to a shot spacing of 100 m. Data were recorded by a 96 channel, 2.4 km long streamer with a 25 m receiver spacing. The resulting common-midpoint (CMP) spacing was 12.5 km and the nominal CMP fold was 12 (Srivastava & Sibuet, 1992).

The processed Erable profiles used in this study are presented as four cross-sections (Figs. 3A to 6A) and the corresponding interpretations (Figs. 3B to 6B) subdivide each of the lines into four crustal domains: continental, transitional, thin oceanic and oceanic. In addition, interpreted deep zones of serpentinized mantle are also highlighted on the interpreted sections. To enable direct comparison with the SCREECH profiles, we also present our modified interpretations of SCR1 and SCR2 (Fig. 7) and show both the uninterpreted data and our interpretation of tieline SCR104 (Fig. 8). A perspective plot of the combined interpretations for all the lines is presented in Figure 9. Before presenting our interpreted subdivisions, we will briefly review the main classification criteria.

5.1 Classification of crustal domains

Extended continental crust at rifted margins is generally characterized by rotated fault blocks, in some places capped with pre-rift sediments. Syn-rift sediments can exhibit growth towards the normal faults that accommodate the movement of the rotated crustal blocks. However, imaging rotated fault blocks alone is not enough evidence to suggest a continental crust affinity because these features are sometimes imaged in ultra-slow spreading ocean crust, such as the Labrador Sea (Srivastava & Keen, 1995). Observing rotated fault blocks in addition to seismic velocities typical of continental crust can provide evidence of a continental crust domain. Continental crustal P-wave velocities generally range from 5.9 to 6.8 km/s (Christensen & Mooney, 1995) and the velocity structure can be described as having a low velocity gradient, between 0.02 and 0.03 km/s based on an average crustal thickness of 38 km.

Normal oceanic crust has an average thickness of 7-8 km and a distinct velocity structure, controlled by the compositional and metamorphic layering that occurs in a typical seafloor-spreading environment (White, 1992). The four-layer classification developed for the oceanic domain consists of sediments (layer 1) with an average P-wave velocity of 2.0 km/s, basalts and sheeted dykes (layer 2) with velocities from 3.5 to 6.6 km/s, gabbro (layer 3) with velocities from 6.5 to 7.2 km/s, and the upper mantle (layer 4) with an average velocity of 8.1 km/s (Christensen & Mooney, 1995). The velocity of layer 4 can be less if the mantle rocks have undergone serpentinization (Horen et al., 1996). The velocity gradient within oceanic crust is approximately 0.5 km/s, much higher than that of continental crust. Ocean crust in slow spreading environments is recognized on seismic reflection data by its rough and highly reflective basement surface, in contrast to the smoother basement surface produced at fast spreading ridges (Malinverno, 1991).

Transitional crust is defined as the domain between extended continental crust and oceanic crust. Four hypotheses have been proposed to explain the nature of transitional crust: 1) highly extended continental crust (Tucholke et al., 1989; Enachescu, 1992; van Avendonk et al., 2006), 2) thin oceanic crust formed by slow or ultra-slow seafloor spreading (Reid, 1994; Keen & de Voogd, 1988; Srivastava et al., 2000), 3) exhumed serpentinized mantle (e.g., Boillot et al. (1987) and Dean et al. (2000)), and 4) a combination of any of the above (e.g., Lau et al. (2006b)). On the Iberian margin, drilling has established that the transitional crust contains exhumed serpentinized mantle (e.g., Boillot et al. (1987), Whitmarsh et al. (1996), Pickup et al. (1996) and Dean et al. (2000)) and this hypothesis has also been proposed to explain the transitional crust on the conjugate Newfoundland margin (e.g., Lau et al. (2006b), Tucholke et al. (2007) and Sibuet et al. (2007a)).

Mantle exhumation can occur during rifting when continental crust becomes extensively thinned and faulted. The extensional faulting allows for seawater to penetrate the upper layer of the mantle, where the seawater reacts with the peridotites and hydrates olivine to serpentine (Pérez-Gussinyé & Reston, 2001; Schroeder et al., 2002). Serpentinization of peridotites changes the physical properties of the rock, producing an increase in volume and a decrease in density. As a result, this decreases the P-wave velocity. The higher the degree of serpentinization, the more the P-wave velocity is reduced. This can result in a wide range of velocities for exhumed mantle that reflects the degree of serpentinization with 8.1 km/s for unaltered mantle, 7.5-7.8 km/s for 10-15% serpentinization and 5 km/s for 100% serpentinization (Christensen & Mooney, 1995; Escartín et al., 2001; Schroeder et al., 2002; Christensen, 2004). Velocities can be even lower if the mafic minerals have been chloritized (Assefa et al., 2000) or if isolated magmatic bodies have been intruded into the mantle (Russell & Whitmarsh, 2003; Cannat et al., 2009). In addition to impacting P-wave velocity, the serpentinization reaction also has a significant effect on the rheological behavior of mantle peridotites with 10% serpentine causing an abrupt reduction in strength (Escartín et al., 2001).

On the Iberian and Galicia Bank margins, transitional crust generally displays a bimodal appearance containing a section of deeper basement with arguably subdued topography adjacent to a series of shallower ridges. The deeper transitional basement is characterized by a velocity structure consisting of an upper layer with low reflectivity less than 3 km thick with velocities ranging between 4.0 and 6.5 km/s (i.e., with a high velocity gradient layer) underlain by a high velocity lower layer with velocities on the order of 7.6 km/s and a low velocity gradient (Dean et al., 2000). Seaward, the shallower basement ridges correspond with a higher velocity range of 6.5 to 7.5 km/s (Dean et al., 2000). To aid in comparing crustal domains across the conjugate margins, we subdivide transitional crust into two sub-domains, T1 and T2, according to whether the transitional basement is deeper with arguably subdued topography or whether it is shallower with distinct peaks that can be interpreted as ridges. For the Newfoundland and Flemish Cap margins, investigating the nature and structure of deep basement within the T1 sub-domain is hampered by the presence of the high amplitude U reflector (Shillington et al., 2008).

5.2 Unstretched continental crust

Several of the Erable profiles investigated in this study extend onto the unstretched crust of the Flemish Cap continental shelf, namely lines E33 (Fig. 3), E53 (Fig. 5) and E36 (Fig. 6). Over the continental shelf, shallow water depth combined with a hard water bottom reflection make noise from multiple reflections a severe problem. Although various multiple removal techniques were used in the processing flow for these profiles, the signal to noise ratio remains very low and basement is detected below the thin sediment layer using refracted arrivals.

Due to the low signal to noise ratio on the continental shelf, intra-crustal reflections are largely absent. However, a small number of discrete reflections are observed between 9 and 10 s at the western end of profile E33, between 9 and 11 s on profile E53 and between 8 and 10 s at the western end of profile E36. These reflections often appear in packages and may correspond to increased lower crustal reflectivity. Since a sharp continuous reflection from the Moho is not observed beneath the continental shelf along any of the profiles, we infer that the Moho coincides with the base of these zones of increased reflectivity. Without alternate Moho depth constraints from seismic refraction surveying, we use the interpreted Moho obtained from a 3-D regional gravity inversion (Welford & Hall, 2007) for comparison. This Moho is time-converted (using regional bathymetric and sediment thickness estimates from the U.S. National Oceanic and Atmospheric Administration, NOAA, and velocities of 1500, 3000 and 6000 m/s for the water, the sediments and the crust respectively) and is overlain as the dark gray line on Figures 3B to 6B. This Moho generally correlates well with the base of the zones of increased reflectivity and discrepancies may be due to our low choice of crustal velocity in the time conversion.

5.3 Stretched continental crust

On all of the profiles considered in this study, the continental slope is characterized by the presence of multiple rotated fault blocks and the continental nature of these blocks is supported by velocity models from nearby seismic refraction experiments (Todd & Reid, 1989; Funck et al., 2003; van Avendonk et al., 2006). The velocity constraints were time-converted and projected along strike to the nearby Erable profiles.

The E33 profile (Fig. 3) is sub-parallel and intersects with SCREECH profile 2 (SCR2; Shillington et al. (2006)) with which it shares many seismic characteristics. The easternmost rotated block (CDPs 11800-13000) coincides with the intersection point with the SCR2 profile (Fig. 9) where this same block is interpreted as the seaward limit of unambiguous thinned continental crust. The only intra-crustal reflections imaged within the continental crust occur within this block and are interpreted as corresponding to the base of pre-rift sediments (Shillington et al., 2006). To the northeast, the E56 profile (Fig. 4) also intersects with SCR2 and exhibits similar seismic reflection characteristics to E33 (Fig. 9) although the rotated fault blocks are poorly imaged. An angular crustal block (CDPs 13800-13400) containing stratigraphic layering that parallels its surface may correlate with similar blocks along E33 and SCR2.

Along the continental slope of profile E54 (Fig. 5), a continental block constrained by velocity model HU-11 (CDPs 10000 to 11000; Todd & Reid (1989)) is similar to a block imaged along SCR1 (Fig. 7A at CDP 56500; Hopper et al. (2004)) and likely supports the same interpretation of a small westward dipping fault block that is bounded by a seaward dipping normal fault to the east. Seaward of this block, three small crustal blocks of unknown origin are present between CDPs 11200 and 13100. Velocity constraints for these blocks are available from the velocity model for HU-18 from Todd and Reid (1989) which contains a 1.5 km thick layer with velocities of 4.5 to 5.0 or 5.1 km/s above a layer with a velocity of 7.1 km/s that increases to approximately 7.3 km/s within 5 km depth. While the velocities for the lower layer are clearly supported by the data, Todd and Reid (1989) used the upper layer velocities from HU-1 and HU-2 for HU-18 since sedimentary and basement refractions were not clearly observed in the data. While the upper layer velocities are consistent with either layer 2 oceanic crust or exhumed serpentinized mantle, they may also represent highly faulted and brecciated continental crust while the lower layer may represent either layer 3 oceanic crust or serpentinized mantle. For this study, the three blocks are interpreted as highly faulted and brecciated continental crust over serpentinized mantle in order to tie in with the interpretation for similar blocks along the intersecting SCR104 profile (Fig. 8). Along SCR104, the same blocks exhibit shallower basement with faulted discontinuities and increased reflectivity compared to the crust to the southwest where transitional crust of the T1 sub-domain has been interpreted and where the U reflector dominates. Further northeast along SCR104 at CDP 95200 (Fig. 8), the basement surface shallows again and exhibits much greater reflectivity that we interpret as the top of thin oceanic crust. The intersection of SCR104 with the toe of thinned continental crust is not surprising given the crooked geometry of the SCR104 profile which jogs in towards Flemish Cap near its intersection point with E54 (Fig. 2B).

Furthest to the northeast, along the continental slope of profile E36 (Fig. 6), several small rotated fault blocks are observed. The crustal block between CDPs 6400 and 6800 is constrained by the velocity structure of an enigmatic block along SCR1 between CDPs 58500 and 60400 (Fig. 7B). Hopper et al. (2004) interpret this block as the seaward limit of continental crust but also suggest that it could correspond to transitional crust in the form of an exhumed peridotite ridge (which would correspond to the T2 sub-domain). While the block along E36 appears geometrically dissimilar to the SCR1 block, in the absence of alternate velocity or other constraints, the block is interpreted as the seaward limit of continental crust, extending the interpretation from Hopper et al. (2004) northeastward. Below this block, projected seismic refraction modelling results (Funck et al., 2003) reveal a pronounced shallowing of the Moho and of the top of the zone of serpentinized mantle which coincide with a prominent landward dipping reflector along E36. This interpreted Moho surface differs significantly from the deeper gravity-inverted Moho which may mean that the thinned crust is of very low density due to extreme faulting or that the upper mantle is of anomalously low density, likely due to serpentinization.

5.4 Transitional crust

5.4.1 Sub-domain T1

Transitional crust sub-domain T1, characterized by deeper basement overlain by the U-reflector, is interpreted along three of the Erable profiles considered in this study. The span of transitional sub-domain T1 is 75 km along E33 (CDPs 11800-5800 in Fig. 3), 40 km along E56 (CDPs 13400-10200 in Fig. 4), and arguably 25 km along profile E54 (CDPs 13100-15300 in Fig. 5). The interpretation of transitional sub-domain T1 crust along profile E54 is based on the presence of the smooth basement uplift at CDP 13500 which exhibits a thin unreflective upper layer over a thicker layer of increased basement reflectivity similar to transitional crust imaged along IAM-9 on the Iberian margin (Pickup et al., 1996). The span of sub-domain T1 along SCR2 is intermediate to that for E33 and E56 at almost 60 km (CDPs 220100-229500 in Fig. 7B) and along the intersecting SCR104 profile, we interpret transitional crust T1 along 100 km of the line (CDPs 102250-118700 in Fig. 8). Overall, these interpretations outline a transitional sub-domain T1 that is widest in the southwest and that pinches out to the northeast.

The nature of transitional sub-domain T1 remains a topic of active debate (Shillington et al., 2006; van Avendonk et al., 2006; van Avendonk et al., 2009). A similar zone has been imaged seismically and successfully drilled on the Iberian margin revealing exhumed serpentinized mantle rocks (Pickup et al., 1996; Dean et al., 2000; Whitmarsh & Wallace, 2001). In the Newfoundland Basin, the zone has not been drilled and the reflective character of the basement cannot be investigated directly due to poor signal penetration through the sills causing the overlying strong U reflection (Shillington et al., 2008). From tomographic inversion of traveltimes picked from seismic refraction data over transitional sub-domain T1 along SCR2, van Avendonk et al. (2006) interpreted the zone as corresponding to thinned continental crust overlying unaltered mantle. In contrast, for the corresponding seismic reflection section along SCR2, Shillington et al. (2006) provided an interpretation of a combination of continental crust with magmatic intrusions/exhumed mantle/thin ocean crust. The initial interpretation of a similar zone along SCR3 to the south (Lau et al., 2006a; Lau et al., 2006b) was similar to that of van Avendonk et al. (2006) with thinned continental crust, although the underlying mantle along SCR3 may be serpentinized. Recently, a reinterpretation of the SCR3 data by Deemer et al. (2009) has identified an exhumed serpentinite diapir within the zone of thinned continental crust identified by Lau et al. (2006a). While this serpentinite diapir occurs landward of several rafted segments of extended continental crust, it may not be isolated feature and may be part of a broader zone of exhumed mantle where the blocks of continental crust are themselves isolated. Such a zone of exhumed mantle with rafted blocks of thinned continental crust has been interpreted on the Iberian margin (Krawczyk et al., 1996; Péron-Pinvidic & Manatschal, 2008) and rafted segments of thinned continental crust may be present within the zones that we have interpreted as transitional sub-domain T1 but they are not imaged.

For transitional sub-domain T1, we prefer an interpretation of exhumed serpentinized mantle, similar to what has been interpreted for the Iberian margin, although we do not rule out the possibility that rafted blocks of thinned continental crust may also exist within this zone. The only available velocity constraints within sub-domain T1 come from the seismic refraction modelling along SCR2 (van Avendonk et al., 2006) where basement velocities increase steadily from 5.5 to 8 km/s. The lower velocity values in this range are not unique to continental rocks and could equally correspond to layer 2 oceanic crust or highly serpentinized exhumed mantle rocks. Furthermore, because wide-angle reflections from the Moho were not included in the modelling of the refraction data from SCR2, the sharpness of the Moho boundary cannot be determined from the velocity model alone and the higher velocity values in the range could equally represent the transition from weakly serpentinized mantle to unaltered mantle. Along profile 54, the smooth basement uplift in the T1 sub-domain (CDP 13500 on Fig. 5) is similar to the interpreted serpentinite diapir on profile SCR3 to the south (Deemer et al., 2009) and may support the same interpretation. The along strike extrapolation of the M3 magnetic anomaly, once considered as a seafloor-spreading anomaly in this region (e.g., Srivastava et al. (2000) and Shipboard Scientific Party (2004)), but now hypothesized to be produced by serpentinized peridotites (Sibuet et al., 2007b), intersects E54 in close proximity to the mound, supporting this interpretation. Seaward of the mound, the sub-domain T1 interpretation is extended to CDP 15000 where it is constrained by the projected velocities from the HU-6 model (Todd & Reid, 1989). This model consists of a 2.5 km thick 4.0-4.5 km/s layer overlying mantle velocities of 7.9-8.0 km/s. These velocity constraints are arguably the most difficult to interpret of all the constraints for the southeastern margin of Flemish Cap. Velocities between 4.0 and 4.5 km/s can equally represent layer 2 oceanic crust or highly serpentinized mantle rocks while velocities within the lower layer can only correspond with unaltered mantle. Todd and Reid (1989) interpreted this model as corresponding to layer 2 oceanic crust directly overlying unaltered mantle at an oceanic fracture zone. While a fracture zone at this location would be consistent with the offset in the M0 chron mapped by Srivastava et al. (2000) and shown in Figure 2B, no evidence for such a zone is imaged in the overlying sedimentary sequence. With serpentinized mantle identified at depth on the profiles to the south and the north as well as landward and seaward along the profile itself, it is difficult to envision a mechanism that would have left this one zone of mantle unaltered. For this reason, the crust constrained by HU-6 is interpreted as exhumed serpentinized mantle corresponding to transitional sub-domain T1. The shallowing of the gravity-inverted Moho beneath the inferred transitional zone may support this interpretation with the inversion compensating for the low density serpentinized mantle by bringing denser unaltered mantle material shallower in the model.

5.4.2 Sub-domain T2

Transitional crust sub-domain T2 is characterized by shallow basement ridges that are most striking and most similar along profiles E56 and SCR2 where they span almost 60 km (CDPs 10250-5650 in Fig. 4 and CDPs 229550-239000 in Fig. 7B). ODP Site 1277 was drilled into a basement high within this sub-domain along profile SCR2 revealing gabbro and basalt fragments along with serpentinized mantle peridotites. Crustal velocity constraints within this sub-domain along profile SCR2 (and projected along strike into the same sub-domain along profile E56) range from 6.0 to 7.8 km/s and are also consistent with an interpretation of exhumed serpentinized mantle peridotites with the degree of serpentinization decreasing with depth (van Avendonk et al., 2006).

The interpreted seaward limit of the T2 sub-domain along profile E56 is constrained by the velocity model for HU-1 and HU-2 (Todd & Reid, 1989) which consists of a 3 km thick basement layer with velocities of 4.5 to 5.0 km/s overlying a 7.3 km/s layer. This velocity model could represent either 1) layer 2 and 3 ocean crust, 2) highly serpentinized and brecciated peridotites (similarly interpreted on IAM-9; Dean et al. (2000)) over moderately serpentinized peridotites, or 3) layer 2 ocean crust over moderately serpentinized peridotite. Todd and Reid (1989) interpreted the velocity model for HU-1 and HU-2 as corresponding to option 1, however later work by Reid (1994) along F85-2 to the south suggested that option 3 might be more appropriate. We adopt the option 3 interpretation to reconcile with the tomographic modeling results along the SCR2 profile where a dramatic increase in the crustal velocity gradient is modelled seaward of M0, consistent with the presence of thin oceanic crust (van Avendonk et al., 2006), and because the velocity of the lower layer is extremely high for layer 3 oceanic rocks and is more likely to represent serpentinized mantle.

Interpreting transitional crust sub-domain T2 along adjacent profiles E33 and E54 is difficult since the basement morphology outboard of transitional sub-domain T1 on both profiles is significantly subdued relative to profiles E56 and SCR2 and since velocity constraints are absent. Nonetheless, the T2 sub-domain interpretation is extended onto profile E33 based on the along strike projection of velocity constraints from SCR2 but the interpretation is limited to a span of less than 20 km (CDPs 5800-4450 in Fig. 3). While it is difficult to justify a different interpretation for sub-domain T2 compared to T1 along E33 without the projected constraints from SCR2, the interpretation has been extended for regional continuity. The landward limit of sub-domain T2 along E33 is placed outboard of the M3 magnetic anomaly, which is associated with serpentinized peridotites (Sibuet et al., 2007b). It could be argued that the western limit of sub-domain T2 could be pushed landward to incorporate the small ridge imaged at CDP 6900 however this ridge intersects with the southwestern limit of the SCR104 profile where the character of the basement more closely resembles transitional sub-domain T1 (Fig. 8B). Along profile E54, we interpret the two basement highs between CDPs 15000 and 16700 (Fig. 5B) as exhumed serpentinized peridotite ridges in order to extend the interpreted regional extent of transitional sub-domain T2 northward. However, this interpretation is purely based on the basement morphology and the seaward extrapolation of the HU-6 velocity model (Todd & Reid, 1989). The basement highs may equally correspond to oceanic crust.

5.5 Thin oceanic crust

Thin oceanic crust attributed to the onset of slow seafloor spreading in a magma-poor environment is interpreted along all the profiles considered in this study with the interpretation heavily dependent on velocity constraints from SCR1 (Funck et al. (2003); Fig. 7A), SCR2 (van Avendonk et al. (2006); Fig. 7B) and velocity model HU-1 and HU-2 from Todd and Reid (1989). At the seaward end of profile E33 (Fig. 3), a velocity profile projected from SCR2 shows velocities ranging from 5.3 to 8.0 km/s with a high velocity gradient consistent with oceanic crust. Within this zone, the basement surface shallows and basement relief becomes rougher. Along the SCR2 profile to the northeast, van Avendonk et al. (2006) interpreted the landward limit of thin oceanic crust near the M0 chron based on a change in the velocity gradient (Fig. 7). Along profile E33, an abrupt boundary between transitional zone T2 and thin oceanic crust is interpreted approximately

45 km inboard of the M0 chron (CDP 1000) but the transition from exhumed serpentinized mantle to thin oceanic crust is likely more gradual with an increasing volume of basaltic material intruded into the transition zone to seaward (Whitmarsh et al., 2001b). Our interpretation implies that slow seafloor spreading began along profile E33 slightly earlier than on the SCR2 and E56 profiles to the northeast.

Along profiles E56 (Fig. 4) and E54 (Fig. 5), the interpretation of thin oceanic crust hinges on the along strike projections of velocity model HU-1 and HU-2 (Todd & Reid, 1989) which consists of a 3 km thick basement layer with velocities of 4.5 to 5.0 km/s overlying a 7.3 km/s layer. This velocity model is similar to velocity profiles at the seaward end of the zone of thin oceanic crust along SCR1 (Fig. 7A) where layer 3 oceanic crust is interpreted to have been pinched out leaving layer 2 oceanic crust directly overlying serpentinized mantle. The lateral extent of thin oceanic crust along profile E56 is limited to 30 km, similar to what is observed on the Galicia Bank margin, based on the interpreted seaward limit of transitional sub-domain T2 and the presence of a domed basement feature (CDPs 3000-2000 in Fig. 4) which we attribute to the onset of normal seafloor spreading. Along profile E54, the lateral extent of thin oceanic crust is 50 km (CDPs 16700 to 21300 in Fig. 5) but this interpretation is poorly constrained. Nonetheless, the zones of thinned oceanic crust on profiles E54 and E56 resemble a similar zone interpreted as thin oceanic crust along SCR1 in terms of both basement morphology and velocity structure (Funck et al., 2003; Hopper et al., 2004).

At the northeastern limit of our study area along profile E36, we interpret thin oceanic crust overlying serpentinized mantle immediately outboard of thinned continental crust based on the rough basement topography and the projected velocity constraints from profile SCR1 (Funck et al. (2003); Fig. 6). Similarly, a zone of thin oceanic crust where layer 2 directly overlies serpentinized mantle is also interpreted to be consistent with that velocity model. The dramatic shallowing of the gravity-inverted Moho along profile E36 (CDPs 8500 to 11500 in Fig. 6) may support this interpretation and may be due to the regional gravity inversion compensating for both the underestimation of the density of the oceanic crust as well as the real shallowing of the Moho.

5.6 Normal oceanic crust

Similar to thin oceanic crust, the interpretation of normal oceanic crust along the Erable profiles relies heavily on velocity constraints from the SCREECH lines (Funck et al., 2003; van Avendonk et al., 2006) although these constraints themselves are highly uncertain since they come from the ends of the profiles where ray coverage is poor. Consequently, our interpretation of normal oceanic crust is poorly constrained and was done by combining the available velocity constraints with changes in basement morphology, a shallower top of basement and increases in crustal reflectivity extending to greater depth. The discrepancy between the deepest basement reflectivity and the shallower gravity-inverted Moho may reflect that over the denser normal oceanic crust, the inversion underestimated the density of the crust and compensated by bringing up denser mantle material.

Normal oceanic crust is interpreted seaward of prominent basement domes along profiles E56 (CDPs 3000 to 2000 in Fig. 4) and E54 (CDPs 21300 to 23000 in Fig. 5). Along profile E54, while the projection of the Aptian-Albian boundary from Tucholke et al. (2007) occurs outboard of the basement dome, we suggest that the dome corresponds with this important boundary and that the boundary should be placed at CDP 21400. Along profile E36, we place the transition from thin oceanic crust to oceanic crust of normal thickness near CDP 11000 based on the projected velocity constraints from SCR1 (Funck et al. (2003); Fig. 7A). Further supporting the thin to normal oceanic crust boundary near CDP 11000 are the moderate increase in basement reflectivity, the shallowing of the basement surface and the increase in basement relief.

5.7 Deep serpentinized mantle

Along all the Erable profiles investigated in this study, deep zones of serpentinized mantle are interpreted on the basis of available velocity constraints. As modelled to the south along profiles SCR3 (Lau et al., 2006a) and FGP85-2 (Reid, 1994), we interpret that serpentinized mantle extends up to 25 km laterally beneath the seaward limit of thinned continental crust based on the velocity models from SCR1 and SCR2 (Funck et al., 2003; van Avendonk et al., 2006). Beneath transitional sub-domain T1 along profiles E33 and E56, we interpret that serpentinized mantle extends at least 2 km beneath the top of basement based on the velocity gradients from SCR2 (van Avendonk et al., 2006) and on where the base of interpreted serpentinized mantle corresponds well with the gravity-inverted Moho. Beneath the interpreted peridotite ridges of transitional sub-domain T2 along profile E56, serpentinized mantle may extend deeper than 4 km based on the available velocity constraints which do not record unaltered mantle velocities (Todd & Reid, 1989; van Avendonk et al., 2006). The base of interpreted serpentinized mantle beneath the ridges is deeper than the gravity-inverted Moho but as with the normal oceanic crust, this discrepancy may reflect that the gravity inversion underestimated the density of the ridges and brought up denser mantle material to compensate. Beneath thin oceanic crust on profiles E36 and E54, serpentinized mantle is interpreted based on the velocity models of HU-1 and HU-2 (Todd & Reid, 1989) and SCR1 (Funck et al., 2003). In contrast, to the south along SCR2, van Avendonk et al. (2006) suggest that the amount of serpentinized mantle beneath the thin oceanic crust is volumetrically limited based on the velocity gradients from their seismic refraction tomography results (van Avendonk et al., 2006) although that velocity model may suffer from poor ray coverage at the end of the line. Overall, a wider interpreted zone of deep serpentinized mantle than that suggested by the lateral extent of exhumed serpentinized mantle at the top of the basement is consistent with what has been interpreted for the Galicia Bank and Iberian margins (Whitmarsh et al., 1996; Dean et al., 2000).

5.8 Evidence for transfer zones?

In order to have accommodated the clock-wise rotation and southeastward motion of Flemish Cap, Sibuet et al. (2007b) postulate that a transfer zone existed south of Flemish Cap. The location of this proposed transfer zone would have been immediately north of and parallel to the SCR2 profile (Fig. 2). The zone of intersection between this transfer zone and profile E33 is highlighted in Figure 3 and falls between CDPs 14500 and 16400 where no obvious structures associated with a transfer zone are imaged by the Erable data apart from a low in the bathymetry which may or may not be related. The zone of intersection between profile E56 and the transfer zone falls within the interpreted transitional T1 sub-domain between CDPs 9700 and 11500 where there is some evidence of increased basement reflectivity but no evidence within the overlying sediments. The intersection of the postulated transfer zone and profile E54 lies in the vicinity of the Aptian-Albian boundary from Tucholke et al. (2007) where once again, no evidence of a transfer zone is observed within the basement or the overlying sediments on the Erable data. The lack of evidence for transfer motion along all the intersecting Erable profiles suggests that if there was motion along the proposed transfer zone, it had to have taken place prior to mantle exhumation and sedimentation.

6 DISCUSSION

6.1 Regional distribution of crustal domains

The interpreted crustal domains from the individual Erable profiles are plotted on a regional bathymetry map in Figure 10 along with corresponding interpretations for nearby SCREECH, FGP and NB profiles. Line drawings of SCR3 and the relevant FGP and NB profiles are plotted in Figure 11 where we have highlighted our interpreted transitional T1 sub-domains. For the profiles lacking velocity constraints (all profiles other than SCR3 and F85-2) and for the poorer data quality NB profiles, we have based our transition zone interpretations on the presence of deep, poorly imaged basement obscured by the U-reflector and on the absence of both imaged fault blocks and significant basement reflectivity. These qualitative interpretations provide a method of tracking the interpreted crustal domains from this study southwestward along the length of the Newfoundland Basin. The interpolated interpretations provide a regional view of the distribution of crustal domains over the Newfoundland and Flemish Cap margins. A similar map for the Galicia Bank and Iberian margins based on the overlain seismic profiles (Fig. 12) and a dense grid of seismic profiles between profiles GP101 and LG12 (Henning et al., 2004) is shown for comparison.

The map views in Figures 10 and 12 illustrate the complexity of the Newfoundland-Iberia and Flemish Cap-Galicia Bank conjugate margins. Along the eastern margins of the Grand Banks and Flemish Cap, a zone of thinned continental crust of variable width exists. On the southeastern margin of Flemish Cap, thinned continental crust narrows from 80 km along E33 and E56 to 50 km along E36 to the northeast. Further south along SCR3, a 170 km wide zone of thinned continental crust (Lau et al., 2006a), the widest on the margin, has recently been reinterpreted and a serpentinite diapir has been identified within the zone of thinned continental crust (Deemer et al., 2009) possibly reducing the width of the zone to 110 km (Fig. 11) if we ignore the outboard rafted blocks of continental crust. Along F85-2 to the south, extended continental crust narrows to 50 km (Reid, 1994) and then appears to widen again along NB21 (Fig. 11).

On the Iberian and Galicia Bank margins, the overall width of the zone of thinned continental crust is greater than the equivalent zone on the Newfoundland and Flemish Cap margins. The widest zone, spanning almost 300 km, corresponds to Galicia Bank. The southern boundary of Galicia Bank may have once corresponded to a transform margin (shown by the transparent brown line labelled TZ1 in Fig. 12) separating it from the Iberian Abyssal Plain to the south. This sharp boundary is hypothesized to have later been obscured by a southward-directed mass wasting event that occurred around the Late Jurassic to Early Cretaceous (Clark et al., 2007). The Iberian Abyssal Plain to the south of this zone of possible mass wasting and the Tagus Abyssal Plain further to the south contain a narrower zone of thinned continental crust on the order of 100 km wide. Between the two abyssal plains at the Estremadura Spur, the width of the zone of thinned continental crust is not known due to the lack of geophysical surveying. For simplicity, we have used the bathymetric contours to interpolate the extent of thinned continental crust between the two abyssal plains, resulting in a zone approximately 150 km wide at this location (Fig. 12).

Outboard of thinned continental crust on the Newfoundland and Flemish Cap margins, two transitional crust sub-domains, T1 and T2, are interpreted. Transitional sub-domain T1, which spans from the southwestern limit of the Newfoundland margin up to profile E54 (Fig. 10), corresponds to deep basement, generally obscured by the U-reflector, which we have interpreted as exhumed serpentinized mantle. The banana-shaped zone varies in width from 20 km along NB21 in the south to between either 80 km (Lau et al., 2006a) and 140 km (Deemer et al., 2009) along SCR3 to 25 km or less along E54 in the northeast. The geometry for the northern half of the zone is constrained by the interpretations presented in Figures 3B to 8B. To constrain the southern half of the zone, we interpreted several NB profiles (Fig. 11) and reinterpreted the velocities within the transition zone along F85-2 from Reid (1994) as corresponding to exhumed serpentinized mantle on the basis of the continuity of the basement character along profile NB26.

On the central Iberian margin, a 70 km wide zone similar to our interpreted transitional sub-domain T1 has been imaged along several seismic profiles. This zone, which appears to narrow to the north toward Galicia Bank (Krawczyk et al., 1996), may have been overridden by a mass wasting event that affected the southern margin of Galicia Bank (Clark et al., 2007) and could be wider than shown in Figure 12 up to the ancient transform boundary. North of the transform boundary along the western margin of Galicia Bank, Henning et al. (2004) find evidence for a narrow zone of exhumed mantle similar to our transitional sub-domain T1 that may underlie the edge of the zone of thinned continental crust. In the Tagus Abyssal Plain further south, Afilhado et al. (2008) used a range of geophysical techniques to investigate the lithospheric structure along a 370 km long W-E transect. They did not find any evidence for exhumed serpentinized mantle or extensive mantle serpentinization below the thin crust but did not rule out the possibility that pockets of serpentinized mantle may exist like those identified on an intersecting 80 km long profile (Pinheiro et al., 1992) and a 100 km long profile to the south (Purdy, 1975).

It is clear that significant along margin variations in mantle exhumation occurred along the Iberian margin. Unfortunately, the gap in seismic coverage and the later emplacement of the Tore Seamount (between 80 and 104 Ma (Merle et al., 2006)) between the IAP and the TAP preclude investigation of the along strike transition from a wide zone of exhumed mantle to no exhumation. As argued in Tucholke and Sibuet (2007), this variation may largely be due to the influence of plume magmatism at the southern end of the margin where the higher temperatures were more conducive to seafloor spreading than mantle exhumation.

On the Newfoundland and Flemish Cap margins, transitional sub-domain zone T2, which is associated with interpreted exhumed serpentinized peridotite ridges, covers a much smaller area than transitional sub-domain T1 and extends along strike less than 100 km to either side of the transfer zone bounding the southwestern margin of Flemish Cap (transparent brown line labelled TZ1 in Fig. 10). With a width perpendicular to strike of approximately 60 km near profiles E56 and SCR2, transitional sub-domain T2 pinches out rapidly to the north and south as interpreted on profiles E33 and E54 (Fig. 10). On the Galicia Bank and Iberian margins, exhumed serpentinized peridotite ridges, equivalent to our transitional sub-domain T2, occur over a greater along strike span and appear to occur further to the south and north than they do on the Newfoundland and Flemish Cap margins (Henning et al., 2004). Curiously, the most poorly developed and difficult to identify ridges on the Galicia Bank margin occur in the vicinity of the transfer zone that defined the ancient southern margin of Galicia Bank and are directly conjugate to the prominent ridges on the Newfoundland-Flemish Cap margins which also straddle the same transfer zone. This coincidence may point to a causal relationship between motion along the transfer zone and the exhumation of shallow peridotite ridges.

A zone of thin oceanic crust varying in width from 30 to 50 km is interpreted to exist outboard of exhumed mantle along the entire length of the Newfoundland and Flemish Cap margins (Fig. 10), although in the absence of direct velocity or drilling constraints the differentiation between transitional sub-domain T2 and thin oceanic crust is subtle. In contrast, for the Galicia Bank and Iberian margins, thin oceanic crust is reported for some seismic refraction profiles (Beslier et al., 1993; Whitmarsh et al., 1993; Sibuet et al., 1995; Whitmarsh et al., 1996) but not for others (Dean et al., 2000; Afilhado et al., 2008) despite their close proximity. For simplicity, we have included a 20 to 30 km wide zone of thin oceanic crust for the Galicia Bank and the central Iberian margins in Figure 12, though this zone is poorly constrained and may show significantly more variability along strike.

With the discovery that serpentinization of exhumed mantle can create the linear seafloor magnetic anomalies classically attributed to seafloor spreading (Sibuet et al., 2007a), magnetic data alone can no longer be used to conclusively identify the onset of normal seafloor spreading and the first instance of oceanic crust of normal thickness. On the Newfoundland and Flemish Cap margins using seismic refraction modelling, the onset of normal seafloor spreading has been loosely constrained at the seaward ends of refraction profiles F85-2, SCR1 and SCR3 (Reid, 1994; Funck et al., 2003; Lau et al., 2006a) but the ray coverage is poor. To generate the regional interpolation of normal oceanic crust in Figure 10, we interpreted normal oceanic crust along the remaining seismic profiles on the basis of both increased basement topography and reflectivity extending to greater depth. To the south of our main study area at the seaward limit of the SCR3 profile, identifying normal oceanic crust is complicated by the presence of the Newfoundland seamounts which were emplaced at 97.7 Ma (Sullivan & Keen, 1977), 25 to 30 million years after seafloor spreading had commenced.

On the Galicia Bank and central Iberian margins, normal oceanic crust has been modelled beyond the zones of exhumed serpentinized mantle at the seaward limit of seismic refraction profiles GP101 and IAM9 (Whitmarsh et al., 1996; Dean et al., 2000). To the south in the Tagus Abyssal Plain along IAM5, Afilhado et al. (2008) have identified normal oceanic crust adjacent to thinned continental crust approximately 200 km inboard of where it occurs to the north. This discrepancy implies that the onset of normal seafloor spreading occurred much earlier in the south than in the north. Due to the lack of deep seismic profiling outboard of the Estremadura Spur and the presence of the prominent Tore Seamount, the details of the along strike variation in the onset of normal seafloor spreading along the Iberian margin, as well as the asymmetry of exposed serpentinite and the presence of thin oceanic crust, cannot be addressed with the available data.

6.2 Reconstruction

In Figure 13, the interpreted crustal domains for the Newfoundland-Flemish Cap and Iberia-Galicia Bank margins are plotted on a modified version of the M0 reconstruction from Sibuet et al. (2007b) and this reconstruction is stepped further back to the M3 chron in Figure 14. Apart from the distinct asymmetries across the conjugate margins and along strike of the individual margins, the most striking feature to stand out from the reconstructions is the compartmentalization of the margins into four along strike regions (identified by Roman numerals I to IV) separated by the flow lines or transfer zones identified by Sibuet et al. (2007b). Each of these along strike regions appears to have undergone a different rifting style than the regions to either side, an observation previously made for the Iberian margin by Whitmarsh et al. (1993). We discuss these four regions from southwest to northeast in the direction of rift propagation, focusing most of our attention on regions III and IV which cover our main study area.

Briefly, region I in the southwest is characterized by asymmetric rifting and/or seafloor spreading which isolated exhumed mantle on the Newfoundland side of the rift zone and focused early seafloor spreading on the Iberian side. On the Iberian side, this early seafloor spreading may have been initiated by nearby plume magmatism (Tucholke & Sibuet, 2007). Region II on the Newfoundland margin is characterized by a wide zone of exhumed serpentinized mantle as evidenced by Deemer et al. (2009) and Figure 11. Region II on the conjugate Iberian margin is poorly understood due to the lack of geophysical surveying but may contain a wider zone of thinned continental crust at the Estremadura Spur compared to the Newfoundland margin. The transfer zones bounding region II on the Iberian margin loosely define the edges of the Estremadura Spur and may have directly influenced its formation by localizing the extensional stresses within the continental crust in this region. On both sides of the North Atlantic, region II was later affected by the emplacement of both the Newfoundland and Tore seamounts.

Region III arguably shows the most symmetry across the conjugate pair, particularly if the material that was mass wasted off the southern boundary of Galicia Bank is restored to its original position and the inferred exhumed serpentinized mantle is exposed at the northern end of the Iberian Abyssal Plain. The main difference between the two sides of region III appears to be the distribution of transitional sub-domain T2 with more of it concentrated on the Iberian side. This may however simply reflect that the final location of breakup did not occur in the centre of the zone of exhumed peridotite ridges.

For the Flemish Cap-Galicia Bank conjugate margins in region IV, the apparent fundamental asymmetry in the amount of thinning experienced by the continental crust can be attributed to several factors. First, while Flemish Cap and Galicia Bank remained connected, much of the thinning on the Newfoundland side was taking place on the other side of Flemish Cap within the Flemish Pass and Orphan Basins as Flemish Cap was rotated out of those basins (Enachescu et al., 2004a; Enachescu et al., 2004b; Enachescu et al., 2004c; Skogseid et al., 2004; Sibuet et al., 2007b). Second, the localization of breakup between Flemish Cap and Galicia Bank occurred closer to the margin of Flemish Cap resulting in the present day asymmetry. Region IV is also unique relative to the regions to the southwest due to the fact that Flemish Cap and Galicia Bank remained attached longer than the other segments of the margin (Tucholke et al., 2007), thus experiencing less exhumation of serpentinized mantle.

6.3 Rifting model

Numerical modelling studies of continental extension, rifting and mantle exhumation (Buck, 1991; Pérez-Gussinyé et al., 2001; Nagel & Buck, 2004; Lavier & Manatschal, 2006; Huismans & Beaumont, 2007), provide the dynamic building blocks from which a simplified temporal rifting evolution model of our study area can be constructed. To explain the range of features observed on the interpreted Erable profiles, the model must be able to explain the lack of imaged large-scale detachments within or at the base of highly thinned continental crust, the bimodal appearance of the transitional basement (sub-domains T1 and T2) interpreted as exhumed serpentinized mantle and the onset of seafloor spreading. This model, which has similarities to the rifting model described by Deemer et al. (2009), is illustrated in Figure 15.

A rheologically stratified lithosphere consisting of a brittle upper crust, a ductile middle crust, a brittle lower crust and a ductile lowermost crust overlying a brittle uppermost mantle/ductile mantle (Pérez-Gussinyé et al., 2001) is subjected to ultraslow extension resulting in the stretching and thinning of continental crust along multiple generations of listric normal faults in the upper, and possibly lower (Brun & Beslier, 1996; Huismans & Beaumont, 2007; Reston, 2007), crust (Fig. 15A). The upper crustal faults sole into ductile middle crustal shear zones which themselves accommodate significant crustal thinning (Whitmarsh et al., 2001a; Nagel & Buck, 2004; Lavier & Manatschal, 2006). Upper and lower crustal brittle faults remain decoupled until the middle crustal shear zones are pinched out (Fig. 15B; Lavier & Manatschal (2006). Eventually, continued thinning and cooling of the crust causes deeper crust to shallow and cool. This cooling depresses the lower crust brittle-ductile transition, strengthening the lowermost crust and coupling it with the uppermost mantle. When the lower crust brittle-ductile transition has reached the crust-mantle boundary, the entire continental crust is embrittled (Pérez-Gussinyé & Reston, 2001). The extreme thinning of the crust and corresponding asthenospheric rise do not result in the production of melt because the extension is so slow and because either the sublithospheric mantle is cool (White et al., 1992; Reston & Phipps Morgan, 2004) and/or partially depleted (Müntener & Manatschal, 2006; Pérez-Gussinyé et al., 2006) or else complete lithospheric separation has not occurred (Minshull et al., 2001).

As ultraslow extension continues, the now completely brittle continental crust becomes thinner, normal faults reach the unaltered mantle below and seawater travels down the faults and serpentinizes the underlying mantle peridotites (Fig. 15B; Pérez-Gussinyé & Reston (2001)). As the underlying mantle becomes increasingly serpentinized and embrittled, continued ultraslow extension causes the serpentinized mantle to be thinned along the faults that have been exposed to the greatest amount of seawater. This enhanced localized faulting of the serpentinized mantle is inferred to occur along multiple mantle shear zones (Nagel & Buck, 2004; Deemer et al., 2009), rather than a large-scale concave-down detachment such as the one proposed by Whitmarsh et al. (2001a) and modelled by Lavier & Manatschal (2006), evidence for which is mostly absent from the Newfoundland and Flemish Cap margins. The multiple mantle shear zones expose deeper mantle to seawater and to further serpentinization while blocks of continental crust get transported outboard (Fig. 15C). This process continues exposing more and more mantle to serpentinization with any rafted blocks of continental crust being pulled further seaward (Fig. 15D) consistent with those presented in Krawczyk et al. (1996), Péron-Pinvidic and Manatschal (2008) and Deemer et al. (2009) .

The mantle that has been exposed to seawater the longest undergoes the greatest amount of serpentinization and consequently the greatest amount of weakening. As proposed by Deemer et al. (2009), such weakened material may be unable to support relief and may have a tendency to flow resulting in the inferred subdued basement surface topography of the transition sub-domain T1 imaged on the seismic profiles considered in this study and others (Krawczyk et al., 1996; Pickup et al., 1996; Lau et al., 2006b; Shillington et al., 2006; Deemer et al., 2009).

An increase in the rate of extension from ultraslow to slow would expose deeper, less serpentinized and stronger mantle peridotites more quickly forming peridotite ridges (Fig. 15E). Such rapid exhumation of ridges would likely be accompanied by the production of melt (Pérez-Gussinyé et al., 2006) which could be incorporated into the ridges and may form the starting point for slow seafloor spreading if this process results in complete lithospheric separation. For the conjugate margins considered in this study, we would argue that the localization of the peridotite ridges in close proximity to the transfer zone between regions III and IV was a direct consequence of abrupt breakup between Flemish Cap and Galicia Bank which occurred later than other segments of the rift. This sudden increase in the extension rate would have exhumed the deeper, less serpentinized mantle peridotites in an area adjacent to the breakup zone limiting their along strike extent. In Figure 15F, basalt is shown extruding among the peridotite ridges at the point of breakup however breakup could occur anywhere that the lithosphere is sufficiently thin due to asthenospheric upwelling (Whitmarsh et al., 2001a).

Along strike variations in rifting style observed across the ancient transfer zones on the Newfoundland-Iberia and Flemish Cap-Galicia Bank conjugate margins may reflect inherited regional variations in structural heterogeneities of the ancient lithosphere as suggested by Huismans & Beaumont (2007). While no evidence for these transfer zones can be found on the individual seismic profiles, meaning that they were no longer active during mantle exhumation and subsequent sedimentation, they appear to have seeded the partitioning of regions with distinct extensional styles along the margins of the North Atlantic. With the transfer zone immediately south of Flemish Cap also postulated to have accommodated its clockwise rotation and southward motion (Sibuet et al., 2007b), ancient transfer zones may play a more significant role in influencing the evolution of the rifting process than is generally acknowledged.

7 CONCLUSIONS

Interpreted multichannel seismic reflection profiles from the 1992 Erable experiment across the southern margin of Flemish Cap into the northern Newfoundland Basin reveal a subdividion of the crust into distinct domains corresponding to thinned continental, transitional (sub-domains T1 and T2), thin oceanic and normal oceanic crust. Combined with results from earlier geophysical surveys, interpolation of these domains across the study region reveals:

- Significant variations in the width of thinned continental crust both along strike and across the conjugate margins.
- A banana-shaped zone of deep transitional basement overlain by the U-reflector and interpreted as exhumed serpentinized mantle that is widest outboard of the central Grand Banks and that pinches out along the southeastern margin of Flemish Cap.

- A localized zone of shallow ridges consisting of exhumed serpentinized mantle peridotites conjugate to a similar zone on the Galicia Bank-Iberia margin. The ridges on both margins straddle a postulated transfer zone that may have accommodated motion of Flemish Cap and defined the ancient southern boundary of Galicia Bank.
- A compartmentalization of rifting styles along the conjugate margins into four distinct along strike regions separated by ancient transfer zones. While the transfer zones were not active during mantle exhumation and seafloor spreading, inherited lithospheric heterogeneities in each of the along strike regions may have seeded the observed along strike variations in rifting styles.

From a model of the temporal evolution of rifting along the margins, the localization of shallow exhumed serpentinized peridotite ridges is attributed to a sudden increase in the rate of extension following the final separation of Flemish Cap and Galicia Bank.

ACKNOWLEDGMENTS

We would like to thank the Geological Survey of Canada and Ifremer for funding the Erable cruise on the CSS Hudson. We would also like to thank the Natural Sciences and Engineering Research Council of Canada for funding in support of this research (NSERC-PDF to Welford and Discovery Grant to Hall). The Atlantic Innovation Fund also provided support to the PanAtlantic Petroleum Systems Consortium (PPSC) which contributed to some of the postdoctoral salary support. Some of the processing software used was donated by Landmark Graphics. We thank John R. Hopper and Tim J. Reston for constructive reviews.

REFERENCES

Abe, N., 2001. Petrochemistry of serpentinized peridotite from the Iberia Abyssal Plain (ODP Leg 173): its character intermediate between suboceanic and subcontinental upper mantle, in *Non-volcanic rifting of continental margins: a comparison of evidence from land and sea*, edited by R. Wilson, R. Whitmarsh, B. Taylor, & N. Froitzheim, vol. 187, pp. 143–159, Geological Society, London.

Afilhado, A., Matias, L., Shiobara, H., Hirn, A., Mendes-Victor, L., & Shimamura, H., 2008. From unthinned continent to ocean: the deep structure of the West Iberia passive continental margin at 38^{circ} n, *Tectonophysics*, **458**(1–4), 9–50.

Assefa, S., McCann, C., & Sothcott, J., 2000. Seismic and petrophysical relationships from UK continental shelf rocks at elevated pressures, *Marine Georesources and Geotechnology*, **18**(2), 119–140.

Beslier, M., Ask, M., & Boillot, G., 1993. Ocean-continent boundary in the Iberia Abyssal Plain from multichannel seismic data, *Tectonophysics*, **218**, 383–393.

Boillot, G. & Winterer, E., 1988. Drilling on the Galicia margin: retrospect and prospect, *Proceedings of the Ocean Drilling Project Scientific Results*, **103**, 809–828.

Boillot, G., Grimaud, S., Mauffret, A., Mougenot, D., Mergoil-Daniel, J., Kornprobst, J., & Torrent, G., 1980. Ocean-continent boundary off the Iberian margin: a serpentinite diapir west of the Galicia Bank, *Earth and Planetary Science Letters*, **48**, 23–34.

Boillot, G., Recq, M., Winterer, E., Meyer, A., Applegate, J., Baltuck, M., Bergen, J., Comas, M., Davies, T., Dunham, K., Evans, C., Girardeau, J., Goldberg, G., Haggerty, J., Jansa, L., Johnson, J., Kasahara, J., Loreau, J., Luna-Sierra, E., Moullade, M., Ogg, J., Sarti, M., Thurow, J., & Williamson, M., 1987. Tectonic denudation of the upper mantle along passive margins: a model based on drilling results (ODP leg 103, western Galicia margin, Spain), *Tectonophysics*, **132**(4), 335–342.

Boillot, G., Girardeau, J., & Kornprobst, J., 1988. Rifting of the Galicia margin: crustal thinning and emplacement of mantle rocks on the seafloor, *Proceedings of the Ocean Drilling Project Scientific Results*, **103**, 741–756.

Bown, J. W. & White, R. S., 1994. Variation with spreading rate of oceanic crustal thickness and geochemistry, *Earth and Planetary Science Letters*, **121**, 435–449.

Brun, J. & Beslier, M., 1996. Mantle exhumation at passive margins, *Earth and Planetary Science Letters*, **142**(1-2), 161–173.

Buck, W. R., 1991. Modes of continental lithospheric extension, *Journal of Geophysical Research*, **96**(B12), 20161–20178.

Cannat, M., Manatschal, G., Sauter, D., & Péron-Pinvidic, G., 2009. Assessing the conditions of continental breakup at magma-poor rifted margins: What can we learn from slow spreading mid-ocean ridges, *Comptes Rendus Geosciences*, **341**(5), 406–427.

Chenet, P., Montadert, L., Gairaud, H., & Roberts, D., 1982. Extension ratio measurements on the Galicia, Portugal and northern Biscay continental margins: implications for evolutionary models of passive continental margins, in *Studies in Continental Margin Geology*, edited by J. Watkins & C. Drake, vol. 34, pp. 703–715, AAPG Memoir.

Chian, D., Louden, K. E., Minshull, T. A., & Whitmarsh, R. B., 1999. Deep structure of the ocean-continent transition in the southern Iberia Abyssal Plain from seismic refraction profiles: Ocean Drilling Program (Legs 149 and 173) transect, *Journal of Geophysical Research*, **104**(B4), 7443–7462.

Christensen, N., 2004. Serpentinites, peridotites, and seismology, *International Geology Review*, **46**(9), 795–816.

Christensen, N. & Mooney, W., 1995. Seismic velocity structure and composition of the continental crust, *Journal of Geophysical Research*, **100**, 9761–9788.

Clark, S. A., Sawyer, D. S., Austin Jr., J. A., Christeson, G. L., & Nakamura, Y., 2007. Characterizing the Galicia Bank-Southern Iberia Abyssal Plain rifted margin segment boundary using multichannel seismic and ocean bottom seismometer data, *Journal of Geophysical Research*, **112**(B03408), doi:10.1029/2006JB004581.

de Charpal, O., Guennoc, P., Montadert, L., & Roberts, D., 1978. Rifting, crustal attenuation and subsidence in the Bay of Biscay, *Nature*, **275**(5682), 706–711.

de Graciansky, P. & Poag, C., 1985. Geologic history of Goban Spur, northwest Europe continental margin, in *Initial Reports of the DSDP*, edited by P. de Graciansky & C. Poag, vol. 80, chap. 58, pp. 1187–1216, US Government Printing Office, Washington, D.C.

Dean, S., Minshull, T., Whitmarsh, R., & Louden, K., 2000. Deep structure of the ocean-continent transition in the southern Iberia Abyssal Plain from seismic refraction profiles: the IAM-9 transect at 40 20'N, *Journal of Geophysical Research*, **105**, 5859–5886.

Deemer, S., Hall, J., Solvason, K., Lau, K. H., Louden, K. E., Srivastava, S., & Sibuet, J.-C., 2009. Structure and development of the southeast Newfoundland continental passive margin: derived from SCREECH Transect 3, *Geophysical Journal International*, **178**(2), 1004–1020.

Enachescu, M. E., 1992. Basement extension on the Newfoundland continental margin (Canadian east coast), in *International Basement Tectonics Association Publication no. 7*, edited by R. Mason, pp. 227–256, Kluwer Academic Publishing.

Enachescu, M. E., 2006. Structural setting and petroleum potential of the Orphan Basin, offshore Newfoundland and Labrador, *Recorder*, **31**(2), 5–13.

Enachescu, M. E., Hogg, J., & Meyer, K., 2004a. East Orphan Basin, offshore Newfoundland and Labrador: A deep water super extended rift with potential petroleum system, in *Canadian Society of Petroleum Geologists (CSPG) Annual Convention, Expanded Abstracts*.

Enachescu, M. E., Kearsey, S., Hogg, J., Einarsson, P., Nader, S., & Smee, J., 2004b. Orphan Basin, offshore Newfoundland, Canada: Structural and tectonic framework, petroleum systems and exploration potential, *Society of Exploration Geophysicists (SEG) 74th Annual Meeting and Exposition, Expanded Abstracts*, **23**(382).

Enachescu, M. E., Meyer, K., & Hogg, J., 2004c. East Orphan Basin: Structural setting and evolution with seismic and potential field arguments, in *Canadian Society of Exploration Geophysicists (CSEG) Annual Convention, Expanded Abstracts*.

Escartín, J., Hirth, G., & Evans, B., 2001. Strength of slightly serpentinized peridotites: implications for the tectonics of oceanic lithosphere, *Geology*, **29**(11), 1023–1026.

Evans, C. & Girardeau, J., 1988. Galicia margin peridotites: undepleted abyssal peridotites from the North

Atlantic, *Proceedings of the Ocean Drilling Project Scientific Results*, **103**, 195–207.

Funck, T., Hopper, J. R., Larsen, H. C., Louden, K. E., Tucholke, B. E., & Holbrook, W. S., 2003. Crustal structure of the ocean-continent transition at Flemish Cap: seismic refraction results, *Journal of Geophysical Research*, **108**(B11), doi:10.1029/2003JB002434.

Girardeau, J., Evans, C., & Beslier, M., 1988. Structural analysis of plagioclase-bearing peridotites emplaced at the end of continental rifting: hole 637A, ODP leg 103 on the Galicia margin, *Proceedings of the Ocean Drilling Project Scientific Results*, **103**, 209–223.

Grant, A. & McAlpine, K., 1990. The continental margin around Newfoundland, in *Geology of the continental margin of Eastern Canada*, edited by M. Keen & G. Williams, chap. 6, pp. 239–292, Geological Survey of Canada, Geology of Canada, no.2.

Haworth, R. & Keen, C. E., 1979. The Canadian Atlantic margin: a passive continental margin encompassing an active past, *Tectonophysics*, **59**, 83–126.

Hébert, R., Gueddari, K., LaFleche, M., Beslier, M., & Gardien, V., 2001. Petrology and geochemistry of exhumed peridotites and gabbros at non-volcanic margins: ODP leg 173 West Iberia ocean-continent transition zone, in *Non-volcanic rifting of continental margins: a comparison of evidence from land and sea*, edited by R. Wilson, R. Whitmarsh, B. Taylor, & N. Froitzheim, vol. 187, pp. 161–189, Geological Society of London, Special Publications.

Henning, A. T., Sawyer, D. S., & Templeton, D. C., 2004. Exhumed upper mantle within the ocean-continent transition on the northern West Iberia margin: evidence from prestack depth migration and total tectonic subsidence analyses, *Journal of Geophysical Research*, **109**(B05103), doi:10.1029/2003JB002526.

Hopper, J., Funck, T., Tucholke, B., Larsen, H. C., Holbrook, W. S., Louden, K. E., Shillington, D. J., & Lau, H., 2004. Continental breakup and the onset of ultraslow seafloor spreading off Flemish Cap on the Newfoundland rifted margin, *Geology*, **32**(1), 93–96.

Hopper, J., Funck, T., Tucholke, B., Louden, K., Holbrook, W., & Larsen, H. C., 2006. A deep seismic investigation of the Flemish Cap margin: implications for the origin of deep reflectivity and evidence for asymmetric break-up between Newfoundland and Iberia, *Geophysical Journal International*, **164**(3), 501–515.

Horen, H., Zamora, M., & Dubuisson, G., 1996. Seismic waves velocities and anisotropy in serpentinized peridotites from Xigaze ophiolite: abundance of serpentine in slow spreading ridge, *Geophysical Research Letters*, **23**(1), 9–12.

Huismans, R. & Beaumont, C., 2007. Roles of lithospheric strain softening and heterogeneity in determining the geometry of rifts and continental margins, in *Imaging, mapping and modelling continental lithosphere extension and breakup*, edited by G. Karner, G. Manatschal, & L. Pinheiro, vol. 282, pp. 111–138, Geological Society of London, Special Publications.

Keen, C. & de Voogd, B., 1988. The continent-ocean boundary at the rifted margin of eastern Canada: new results from deep seismic reflection studies, *Tectonics*, **7**, 107–124.

Keen, C. E., Boutilier, R., de Voogd, B., Mudford, B., & Enachescu, M. E., 1987. Crustal geometry and extensional models for the Grand Banks, eastern Canada: constraints from deep seismic reflection data, in *Sedimentary Basins and Basin-Forming Mechanisms*, edited by C. Beaumont & A. Tankard, vol. 12, pp. 101–115, Canadian Society of Petroleum Geologists.

King, L., Fader, G., Poole, W., & Wanless, R., 1985. Geological setting and age of the Flemish Cap granodiorite, east of the Grand Banks of Newfoundland, *Canadian Journal of Earth Sciences*, **22**, 1286–1298.

Kornprobst, J. & Tabit, A., 1988. Plagioclase-bearing ultramafic tectonics from the Galicia margin (leg 103, site 637): comparison of their origin and evolution with low-pressure ultramafic bodies in western Europe, *Proceedings of the Ocean Drilling Project Scientific Results*, **103**, 253–268.

Krawczyk, C., Reston, T., Beslier, M., & Boillot, G., 1996. Evidence for detachment tectonics on the Iberia Abyssal Plain rifted margin, *Proceedings of the Ocean Drilling Project Scientific Results*, **149**, 603–615.

Lau, K. H., Louden, K. E., Funck, T., Tucholke, B. E., Holbrook, W. S., Hopper, J. R., & Larsen, H. C., 2006a. Crustal structure across the Grand Banks-Newfoundland Basin continental margin - I. Results from a seismic refraction profile, *Geophysical Journal International*, **167**, 127–156.

Lau, K. H., Louden, K. E., Deemer, S., Hall, J., Hopper, J. R., Tucholke, B. E., Holbrook, W. S., & Larsen, H. C., 2006b. Crustal structure across the Grand Banks-Newfoundland Basin continental margin - II. Results from a seismic reflection profile, *Geophysical Journal International*, **167**, 157–170.

Lavier, L. & Manatschal, G., 2006. A mechanism to thin the continental lithosphere at magma-poor margins, *Nature*, **440**(7082), 324–328.

Le Pichon, X., Sibuet, J.-C., & Francheteau, J., 1977. The fit of continent around the North Atlantic Ocean, *Tectonophysics*, **38**, 169–209.

Louden, K. E. & Chian, D., 1999. The deep structure of non-volcanic rifted continental margins, *Philosophical transactions of the Royal Society of London*, **357**, 767–804.

Malinverno, A., 1991. Inverse square-root dependence of mid-ocean flank roughness on spreading rate, *Nature*, **352**, 58–60.

Mauffret, A., Mougenot, D., Miles, P., & Malod, J., 1989. Cenozoic deformation and Mesozoic abandoned spreading centre in the Tagus Abyssal Plain (west of Portugal): results of a multichannel seismic survey, *Canadian Journal of Earth Sciences*, **26**, 1101–1123.

Merle, R., Schärer, U., Girardeau, J., & Cornen, G., 2006. Cretaceous seamounts along the continent-ocean transition of the Iberian margin: U-Pb ages and Pb-Sr-Hf isotopes, *Geochimica et Cosmochimica Acta*, **70**, 4950–4976.

Minshull, T., Dean, S., White, R., & Whitmarsh, R., 2001. Anomalous melt production after continental break-up in the southern Iberia Abyssal Plain, in *Non-volcanic rifting of continental margins: a comparison of evidence from land and sea*, edited by R. Wilson, R. Whitmarsh, B. Taylor, & N. Froitzheim, vol. 187, pp. 537–550, Geological Society, London.

Montadert, L., de Charpal, O., Roberts, D., Guennoc, P., & Sibuet, J.-C., 1979. Northeast Atlantic passive continental margin: rifting and subsidence processes, in *Deep Drilling Results in the Atlantic Ocean: continental margins and paleoenvironment*, edited by M. Talwani, W. Hay, & W. Ryan, vol. 3 of **Maurice Ewing Series**, pp. 154–186, AGU, Washington, D.C.

Mougenot, D., Kidd, R., Mauffret, A., Regnauld, H., Rothwell, R., & Vanney, J., 1984. Geological interpretation of combined Sea Beam, GLORIA, and seismic data from Porto and Vigo Seamounts, Iberian continental margin, *Marine Geophysical Researches*, **6**(4), 329–353.

Müntener, O. & Manatschal, G., 2006. High degrees of melt extraction recorded by spinel harzburgite of the Newfoundland margin: the role of inheritance and consequences for the evolution of the southern North Atlantic, *Earth and Planetary Science Letters*, **252**(3–4), 437–452.

Murillas, J., Mougenot, D., Boillot, G., Comas, M., Banda, E., & Mauffret, A., 1990. Structure and evolution of the Galicia Interior Basin (Atlantic western Iberian continental margin), *Tectonophysics*, **184**(3–4), 297–319.

Nagel, T. J. & Buck, W., 2004. Symmetric alternative to asymmetric rifting models, *Geology*, **32**, 937–940.

Pérez-Gussinyé, M. & Reston, T., 2001. Rheological evolution during extension at nonvolcanic rifted margins: onset of serpentinization and development of detachments leading to continental breakup, *Journal of Geophysical Research*, **106**(B3), 3961–3975.

Pérez-Gussinyé, M., Reston, T., & Phipps Morgan, J., 2001. Serpentinization and magmatism during extension at non-volcanic margins: the effect of initial lithospheric structure, in *Non-volcanic rifting of continental margins: a comparison of evidence from land and sea*, edited by R. Wilson, R. Whitmarsh, B. Taylor, & N. Froitzheim, vol. 187, pp. 551–576, Geological Society of London, Special Publications.

Pérez-Gussinyé, M., Morgan, J., Reston, T., & Ranero, C., 2006. The rift to drift transition at non-volcanic margins: insights from numerical modelling, *Earth and Planetary Science Letters*, **244**(1–2), 458–473.

Péron-Pinvidic, G. & Manatschal, G., 2008. The final rifting evolution at deep magma-poor passive margins from Iberia-Newfoundland: a new point of view, *International Journal of Earth Sciences*, **doi:10.1007/s00531-008-0337-9**.

Pickup, S., Whitmarsh, R., Fowler, C., & Reston, T., 1996. Insight into the nature of the ocean-continent transition off West Iberia from a deep multichannel seismic reflection profile, *Geology*, **24**, 1079–1082.

Pinheiro, L., Whitmarsh, R., & Miles, P., 1992. The ocean-continent boundary off the western continental margin of Iberia, I. Crustal structure in the Tagus Abyssal Plain, *Geophysical Journal International*, **109**(1), 106–124.

Pinheiro, L., Wilson, R., dos Reis, R., Whitmarsh, R., & Ribeiro, A., 1996. The western Iberia margin: a geophysical and geological overview, *Proceedings of the Ocean Drilling Project Scientific Results*, **149**, 3–23.

Purdy, G., 1975. The eastern end of the Azores-Gibraltar plate boundary, *Geophysical Journal of the Royal Astronomical Society*, **43**(3), 973–1000.

Reid, I., 1994. Crustal structure of a nonvolcanic rifted margin east of Newfoundland, *Journal of Geophysical Research*, **99**(B8), 15161–15180.

Reid, I. & Keen, C. E., 1990a. High seismic velocities associated with reflections from within the lower oceanic crust near the continental margin of eastern Canada, *Earth and Planetary Science Letters*, **99**, 118–126.

Reid, I. & Keen, C. E., 1990b. Deep crustal structure beneath a rifted basin: results from seismic refraction measurements across the Jeanne d'Arc Basin, offshore eastern Canada, *Canadian Journal of Earth Sciences*, **27**, 1462–1471.

Reston, T., 1996. The S reflector west of Galicia: the seismic signature of a detachment fault, *Geophysical Journal International*, **127**, 230–244.

Reston, T., 2007. Extension discrepancy of North Atlantic nonvolcanic rifted margin: depth-dependent stretching or unrecognized faulting?, *Geology*, **35**(4), 367–370.

Reston, T. & Phipps Morgan, J., 2004. The continental geotherm and the evolution of rifted margins, *Geology*, **32**, 133–136.

Reston, T., Krawczyk, C., & Klaeschen, D., 1996. The S reflector west of Galicia (Spain): evidence from prestack depth migration for detachment faulting during continental breakup, *Journal of Geophysical Research*, **101**, 8075–8092.

Russell, S. & Whitmarsh, R., 2003. Magmatism at the west Iberia non-volcanic rifted continental margin: evidence from analyses of magnetic anomalies, *Geophysical Journal International*, **154**(3), 706–730.

Schroeder, T., John, B., & Frost, B., 2002. Geologic implications of seawater circulation through peridotite exposed at slow-spreading mid-ocean ridges, *Geology*, **30**(4), 367–370.

Shillington, D. J., Holbrook, W., Tucholke, B., Hopper, J. R., Louden, K. E., Larsen, H. C., van Avendonk, H. J., Deemer, S., & Hall, J., 2004. Data report: marine geophysical data on the Newfoundland nonvolcanic rifted margin around SCREECH transect 2, *Proceedings of the Ocean Drilling Program, Initial Reports*, **210**, 1–36.

Shillington, D. J., Holbrook, W. S., van Avendonk, H. J., Tucholke, B. E., Hopper, J. R., Louden, K. E., Larsen, H. C., Nunes, G. T., & Party, O. L. . S., 2006. Evidence for asymmetric nonvolcanic rifting and slow incipient oceanic accretion from seismic refraction data on the Newfoundland margin, *Journal of Geophysical Research*, **111**(B09402), doi:10.1029/2005JB003981.

Shillington, D. J., Tucholke, B. E., Karner, G., Sawyer, D., Holbrook, W. S., & Delius, H., 2007. Linking core and seismic data without logs: core-seismic correlation at Site 1276, *Proceedings of the Ocean Drilling Project Scientific Results*, **210**, 1–33.

Shillington, D. J., Hopper, J. R., & Holbrook, W., 2008. Seismic signal penetration beneath post-rift sills on the Newfoundland rifted margin, *Geophysics*, **73**(5), B99–B107.

Shipboard Scientific Party, 1979. *Volume XLVII Part 2*, chap. Introduction and explanatory notes, pp. 5–22, Deep Sea Drilling Program.

Shipboard Scientific Party, 1987. Introduction, objectives, and principal results: Ocean Drilling Program leg 103, west Galicia margin, *Proceedings of the Ocean Drilling Program, Initial Reports*, **103**, 3–17.

Shipboard Scientific Party, 1998. Leg 173 introduction, *Proceedings of the Ocean Drilling Program, Initial Reports*, **173**, 7–23.

Shipboard Scientific Party, 2003. Drilling the Newfoundland half of the Newfoundland-Iberia transect: the first conjugate margin drilling in a nonvolcanic rift, *Leg 210 Preliminary Report, Ocean Drilling Program*, **110**.

Shipboard Scientific Party, 2004. Leg 210 summary, *Proceedings of the Ocean Drilling Program, Initial Reports*, **210**, 1–78.

Sibuet, J.-C., Louvel, V., Whitmarsh, R. B., White, R. S., Horsefield, S. J., Sichler, B., Léon, P., & Recq, M., 1995. Constraints on rifting processes from refraction and deep-tow magnetic data: the example of the Galicia continental margin (west Iberia), in *Rifted ocean-continent boundaries*, edited by E. Banda, M. Torné, & M. Talwani, vol. 463 of **NATO ASI Series, Series C: Mathematical and Physical Sciences**, pp. 197–217, Kluwer Academic Publishers.

Sibuet, J.-C., Srivastava, S., & Spakman, W., 2004. Pyrenean orogeny and plate kinematics, *Journal of Geophysical Research*, **109**(B08104), doi:10.1029/2003JB002514.

Sibuet, J.-C., Srivastava, S., & Manatschal, G., 2007a. Exhumed mantle-forming transitional crust in the Newfoundland-Iberia rift and associated magnetic anomalies, *Journal of Geophysical Research*, **112**(B06105), doi:10.1029/2005JB003856.

Sibuet, J.-C., Srivastava, S., Enachescu, M. E., & Karner, G., 2007b. Early Cretaceous motion of Flemish Cap with respect to North America: implications on the formation of Orphan Basin and SE Flemish Cap-Galicia Bank conjugate margins, in *Imaging, mapping and modelling continental lithosphere extension and breakup*, edited by G. Karner, G. Manatschal, & L. Pinheiro, vol. 282, pp. 63–76, Geological Society of London, Special Publications.

Skogseid, J., Barnwell, A., Aarseth, E., Alsgaard, P., Briseid, H., & Zwach, C., 2004. Orphan basin: Multiple failed rifting during early opening of the north Atlantic, *Eos, Transactions of the American Geophysical Union, Joint Assembly Supplement*, **85**(T41B-03).

Srivastava, S. & Keen, C., 1995. A deep seismic reflection profile across the extinct Mid-Labrador Sea spreading center, *Tectonics*, **14**, 372–389.

Srivastava, S. & Sibuet, J.-C., 1992. A joint AGC and IFREMER geophysical cruise to the Newfoundland and Orphan Basins, Cruise Report CSS Hudson 92-22 Mission Erable (Unpublished Report), 121 pp., Geological Survey of Canada, Dartmouth, N.S. and Institut Français de Recherche pour l'Exploitation de la Mer, Centre de Brest.

Srivastava, S. & Verhoef, J., 1992. Evolution of Mesozoic sedimentary basins around the North Central Atlantic: a preliminary plate kinematic solution, in *Basins on the Atlantic Seaboard: petroleum geology, sedimentology and basin evolution*, edited by J. Parnell, vol. 62, pp. 397–420, Geological Society, London.

Srivastava, S., Roest, W., Kovacs, L., Oakey, G., Lévesque, S., Verhoef, J., & Macnab, R., 1990. Motion of Iberia since the Late Jurassic: Results from detailed aeromagnetic measurements in the Newfoundland Basin, *Tectonophysics*, **184**(3–4), 229–260.

Srivastava, S., Sibuet, J.-C., Cande, S., Roest, W., & Reid, I., 2000. Magnetic evidence for slow seafloor spreading during the formation of the Newfoundland and Iberian margins, *Earth and Planetary Science Letters*, **182**(1), 61–76.

Sullivan, K. & Keen, C., 1977. Newfoundland Seamounts - petrology and geochemistry, in *Volcanic regimes of Canada*, edited by W. Baragar, L. Coleman, & J. Hall, vol. 16, pp. 461–476, Geological Association of Canada.

Todd, B. & Reid, I., 1989. The continent-ocean boundary south of Flemish Cap: constraints from seismic refraction and gravity, *Canadian Journal of Earth Sciences*, **26**, 1392–1407.

Tucholke, B. & Sibuet, J.-C., 2007. Leg 210 synthesis: tectonic, magmatic and sedimentary evolution of the Newfoundland-Iberia rift, *Proceedings of the Ocean Drilling Project Scientific Results*, **210**, 1–56.

Tucholke, B., Austin, J., & Uchupi, E., 1989. Crustal structure and rift-drift evolution of the Newfoundland basin, in *Extensional tectonics and stratigraphy of the North Atlantic margins*, edited by A. Tankard & H. Balkwill, vol. 46, chap. 16, pp. 247–263, AAPG Memoir.

Tucholke, B., Sawyer, D., & Sibuet, J.-C., 2007. Breakup of the Newfoundland-Iberia rift, in *Imaging, mapping and modelling continental lithosphere extension and breakup*, edited by G. Karner, G. Manatschal, & L. Pinheiro, vol. 282, pp. 9–46, Geological Society of London, Special Publications.

van Avendonk, H. J., Holbrook, W. S., Nunes, G. T., Shillington, D. J., Tucholke, B. E., Louden, K. E., Larsen, H. C., & Hopper, J. R., 2006. Seismic velocity structure of the rifted margin of eastern Grand Banks of Newfoundland, Canada, *Journal of Geophysical Research*, **111**(B11404), doi:10.1029/2005JB004156.

van Avendonk, H. J., Lavier, L. L., Shillington, D. J., & Manatschal, G., 2009. Extension of continental crust at the margin of the eastern Grand Banks, Newfoundland, *Tectonophysics*, **468**(1–4), 131–148.

Welford, J. K. & Hall, J., 2007. Crustal structure across the Newfoundland rifted continental margin from constrained 3-D gravity inversion, *Geophysical Journal International*, **171**, 890–908.

White, R., 1992. Crustal structure and magmatism of North Atlantic continental margins, *Journal of the Geological Society, London*, **149**, 841–854.

White, R., McKenzie, D., & O'Nions, R., 1992. Oceanic crustal thickness from seismic measurements and rare earth element inversions, *Journal of Geophysical Research*, **97**(B13), 19683–19715.

Whitmarsh, R. & Wallace, P., 2001. The rift-to-drift development of the west Iberia nonvolcanic continental margin: A summary and review of the contribution of ocean drilling program leg 173, *Proceedings of the Ocean Drilling Project Scientific Results*, **173**, 1–36.

Whitmarsh, R., Miles, P., & Mauffret, A., 1990. The ocean-continent boundary off the western continental margin of Iberia, I. Crustal structure at 40 30'N, *Geophysical Journal International*, **103**, 509–531.

Whitmarsh, R., Pinheiro, L., Miles, P., Recq, M., & Sibuet, J.-C., 1993. Thin crust at the western Iberia ocean-continent transition and ophiolites, *Tectonics*, **12**(5), 1230–1239.

Whitmarsh, R., White, R. S., Horsefield, S. J., Sibuet, J.-C., Recq, M., & Louvel, V., 1996. The ocean-continent boundary off the western continental margin of Iberia: crustal structure west of Galicia Bank, *Journal of Geophysical Research*, **101**(B12), 28291–28314.

Whitmarsh, R., Dean, S., Minshull, T., & Tompkins, M., 2000. Tectonic implications of exposure of lower continental crust beneath the Iberia Abyssal Plain, Northeast Atlantic Ocean: geophysical evidence, *Tectonics*, **19**, 919–942.

Whitmarsh, R., Manatschal, G., & Minshull, T., 2001a. Evolution of magma-poor continental margins from rifting to seafloor spreading, *Nature*, **413**(6852), 150–154.

Whitmarsh, R., Minshull, T., Russell, S., Dean, S., Louden, K., & Chian, D., 2001b. The role of syn-rift magmatism in the rift-to-drift evolution of the west Iberia continental margin: geophysical observations, in *Non-volcanic rifting of continental margins: a comparison of evidence from land and sea*, edited by R. Wilson, R. Whitmarsh, B. Taylor, & N. Froitzheim, vol. 187, pp. 107–124, Geological Society of London, Special Publications.

Williams, H., 1984. Miogeoclines and suspect terranes of the Caledonian-Appalachian orogen: tectonic patterns in the North Atlantic region, *Canadian Journal of Earth Sciences*, **21**(887–901).

Williams, H., 1995. *Geology of the Appalachian-Caledonian orogen in Canada and Greenland*, Geological Survey of Canada, Geology of Canada, no.6.

8 FIGURE CAPTIONS

Fig. 1. Bathymetric map of the North Atlantic region, adapted from Chian et al. (1999). Locations of magnetic anomalies M0, M3 and 34 (from Srivastava et al. (1990) and (2000)) are plotted as dotted line segments respectively. Red boxes correspond to our study area offshore Newfoundland and the Iberian region used for comparison with our results. Abbreviations: GB-Grand Banks; FC-Flemish Cap; NB-Newfoundland Basin; GAL-Galicia Bank; IAP-Iberia Abyssal Plain; TAP-Tagus Abyssal Plain; GS-Goban Spur; LAB-Labrador margin; SWG-Southwest Greenland margin; FZ-fracture zone.

Fig. 2 Bathymetric map of study region (A) with enlarged view of Flemish Cap region in (B). A detailed plot of the specific portions of multichannel seismic reflection profiles considered in detail in this study is shown in (C) with regular CDP locations labelled. In (A) and (B), multichannel seismic reflection profiles are plotted with solid black lines corresponding to the Erable experiment (lines E33, E36, E53, E54 and E56), dashed black lines corresponding to the SCREECH experiment (lines SCR1, SCR2, SCR3 and SCR104; (Funck et al., 2003; Hopper et al., 2004; Lau et al., 2006a; Lau et al., 2006b; Shillington et al., 2006; van Avendonk et al., 2006)), solid gray lines corresponding to the Frontier Geoscience Project (lines F85-2, F85-3 and F85-4; (Keen et al., 1987; Keen & de Voogd, 1988; Reid & Keen, 1990a; Reid & Keen, 1990b; Reid, 1994)) and dashed gray lines corresponding to the Newfoundland Basin experiment (lines NB1, NB3, NB4, NB8, NB19, NB21 and NB26; (Tucholke et al., 1989)). Solid blue lines in (B) correspond to the refraction lines from Todd and Reid (1989). Locations of magnetic anomalies M0 and M3 identified by Srivastava et al. (2000) are plotted in (B) as red and purple line segments respectively. Circled numbers 6 and 7 in (A) and (B) correspond to locations of ODP drillholes 1276 and 1277 respectively. In (C), the Erable and SCREECH profiles are plotted as black and grey lines, respectively. Key bathymetric features are labelled in gray. Abbreviations: NNFB-Northern Newfoundland Basin; SNFB-Southern Newfoundland Basin; Nfld-Newfoundland; TFZ-transfer zone.

Fig. 3. (A) Time migration of the Erable 33 (E33) seismic reflection profile with the corresponding

interpretation of crustal domains (B). The legend to the right of the figure explains the shading and line colours used in the interpretation. The locations of magnetic anomalies M0 and M3 identified by Srivastava et al. (2000) are shown at the bottom of the sections. Crossovers with other seismic lines and projected ODP sites are identified with black arrows. The zone of overlap with the transfer zone discussed by Sibuet et al. (2007b) is highlighted with the double-pointed gray arrow. In B, the overlain vertical velocity profiles were projected from the OBS locations in Figure 7B. The dark gray line corresponds to time-converted Moho constraints obtained from the 3-D regional gravity inversion from Welford and Hall (2007). The interpretations of crustal boundaries, labelled along the bottom of plot B, are discussed in the text. Abbreviations: U-U reflection.

Fig. 4. (A) Time migration of the Erable 56 (E56) seismic reflection profile with the corresponding interpretation of crustal domains (B). Refer to the legend in Figure 3 for explanation of shading and line colours in B. In B, the overlain vertical velocity profiles were projected from the lines from Todd and Reid (1989) and the OBS locations in Figure 7B. Remaining caption as in Figure 3.

Fig. 5. (A) Time migration of the combined Erable 53 and 54 (E53 and E54) seismic reflection profiles with the corresponding interpretation of crustal domains (B). Refer to the legend in Figure 3 for explanation of shading and line colours in B. Crossovers with other seismic lines and the Aptian-Albian boundary from Tucholke et al. (2007) are identified with black arrows. In B, the overlain vertical velocity profiles were projected from the lines from Todd and Reid (1989) and the OBS locations in Figure 7B. Remaining caption as in Figure 3.

Fig. 6. (A) Time migration of the Erable 36 (E36) seismic reflection profile with the corresponding interpretation of crustal domains (B). Refer to the legend in Figure 3 for explanation of shading and line colours in B. In B, the overlain vertical velocity profiles were projected from the OBS locations in Figure 7A. Abbreviations: M-Moho. Remaining caption as in Figure 3.

Fig. 7. Interpretations of time migrations for SCREECH lines 1 and 2, SCR1 (A) and SCR2 (B). Refer to the legend in Figure 3 for explanation of shading and line colours. The locations of magnetic anomalies M0 and M3 identified by Srivastava et al. (2000) and crossovers with other seismic lines are identified with black arrows. Numbered red circles along the sea bottom in both plots correspond to ocean-bottom seismometer (OBS) locations for the seismic refraction profiles presented in Funck et al. (2003) and van Avendonk et al. (2006). The overlain vertical velocity profiles were obtained from those studies. The crustal domain interpretations were adapted and reinterpreted from Hopper et al. (2004) and Shillington et al. (2006) to correspond with the interpretations for the Erable profiles.

Fig. 8. (A) Time migration of the SCREECH 104 (SCR104) seismic reflection profile with the corresponding interpretation of crustal domains (B). Refer to the legend in Figure 3 for explanation of shading and line colours in B. In B, the overlain vertical velocity profiles were projected from the OBS locations in Figure 7. Remaining caption as in Figure 3.

Fig. 9. Perspective plot of the interpretations for E33, E36, E54, E56, SCR1, SCR2 and SCR104 showing spatial relationship between the lines. Interpreted crustal domains correspond to those labelled in Figures 3 to 6. Refer to the legend in Figure 3 for explanation of shading and line colours. Vertical scale of slices in two-way traveltime (s) is shown on the slice for E56.

Fig. 10. Map of project area showing bathymetry (gray contours) and the interpreted crustal boundaries and domains from the Erable, SCREECH, FGP and NB profiles considered in this study with seismic line descriptions as in the caption of Figure 2. The locations of magnetic anomalies M0 and M3 are taken from Srivastava et al. (2000) and the location of the Aptian-Albian boundary is taken from Tucholke et al. (2007). The thick black lines and the transparent brown lines correspond to the hinge and flow lines (transfer zones?), respectively, identified by Sibuet et al. (2007b). The areal extent of the more recent Newfoundland seamounts is also shown. Abbreviations: NNFB-

Northern Newfoundland Basin; SNFB-Southern Newfoundland Basin; TZ-transfer zone.

Fig. 11. Line drawings for time migrations of seismic reflection sections along the southern Newfoundland margin from the NB, FGP and SCREECH projects which are used to extend our interpretation of transitional zone T1 to the south. On each section, crossovers with other seismic lines are identified with black arrows The map in A shows the line locations along with our areal interpolation of transitional zone T1 between the lines. The areal extent of the more recent Newfoundland (Nfld) seamounts is also shown.

Fig. 12. Map of Galicia Bank and Iberian margins showing bathymetry (gray contours) and the interpreted crustal boundaries and domains from the overlain seismic profiles, GP101 (Whitmarsh et al., 1996), IAM5 (Afilhado et al., 2008), IAM9 (Dean et al., 2000), ISE9 (Clark et al., 2007), LG12 (Krawczyk et al., 1996), LG14 (Pickup et al., 1996) and a number of seismic lines between GP101 and LG12 (Henning et al., 2004). The locations of magnetic anomalies M0 and M3 are taken from Srivastava et al. (2000) and the location of the Aptian-Albian (Apt-Alb) boundary is taken from Tucholke et al. (2007). The thick black lines and the transparent brown lines correspond to the hinge and flow lines (transfer zones?), respectively, identified by Sibuet et al. (2007b). The areal extents of the more recent Tore Seamount (TS) and Madeira-Tore Rise (MTR) are also shown. Abbreviations: ES-Estremadura Spur; GAL-Galicia Bank; IAP-Iberia Abyssal Plain; TAP-Tagus Abyssal Plain; TZ-transfer zone.

Fig. 13. Interpreted crustal boundaries and domains for both the Newfoundland-Flemish Cap and Iberia-Galicia Bank margins on the M0 reconstruction from Sibuet et al. (2007b). The locations of magnetic anomalies M0 and M3 are taken from Srivastava et al. (2000). Roman numerals correspond to regions discussed in the text. Abbreviations: NNFB-Northern Newfoundland Basin; SNFB-Southern Newfoundland Basin; GAL-Galicia Bank; GIB-Galicia Interior Basin; IAP-Iberia Abyssal Plain; ES-Estremadura Spur; TAP-Tagus Abyssal Plain; FC-Flemish Cap; FPB-Flemish Pass Basin; JAB-Jeanne d'Arc Basin; WOB-West Orphan Basin; EOB-East Orphan Basin; OK-

Orphan Knoll; BB-Bay of Biscay; GS-Goban Spur; PSB-Porcupine-Seabight Basin; PB-Porcupine Bank; RT-Rockall Trough; FZ-Fault Zone.

Fig. 14. Interpreted crustal boundaries and domains for both the Newfoundland-Flemish Cap and Iberia-Galicia Bank margins lined up approximately along the M3 magnetic anomaly from Srivastava et al. (2000). Legend and remaining caption as in Figure 13.

Fig. 15. Diagram of the temporal evolution of the rift model. Explanation of diagram provided in the text.

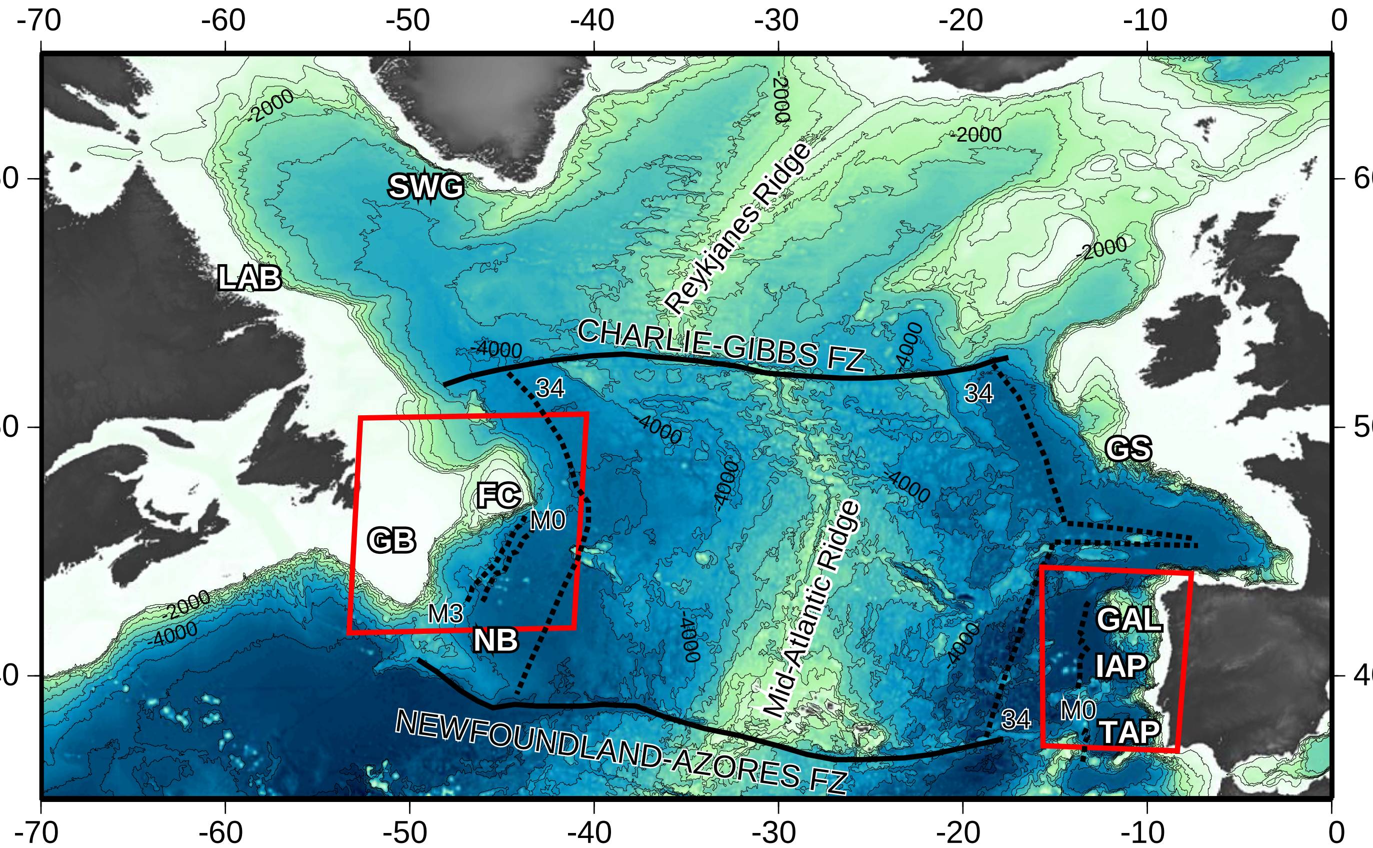

-70
-60
-50
-40
-30
-20
-10
0
60
50
40
-2000
-4000
SWG
LAB
Reykjanes Ridge
CHARLIE-GIBBS FZ
34
GS
FC
M0
GB
M3
NB
Mid-Atlantic Ridge
GAL
IAP
TAP
NEWFOUNDLAND-AZORES FZ

Figure 1

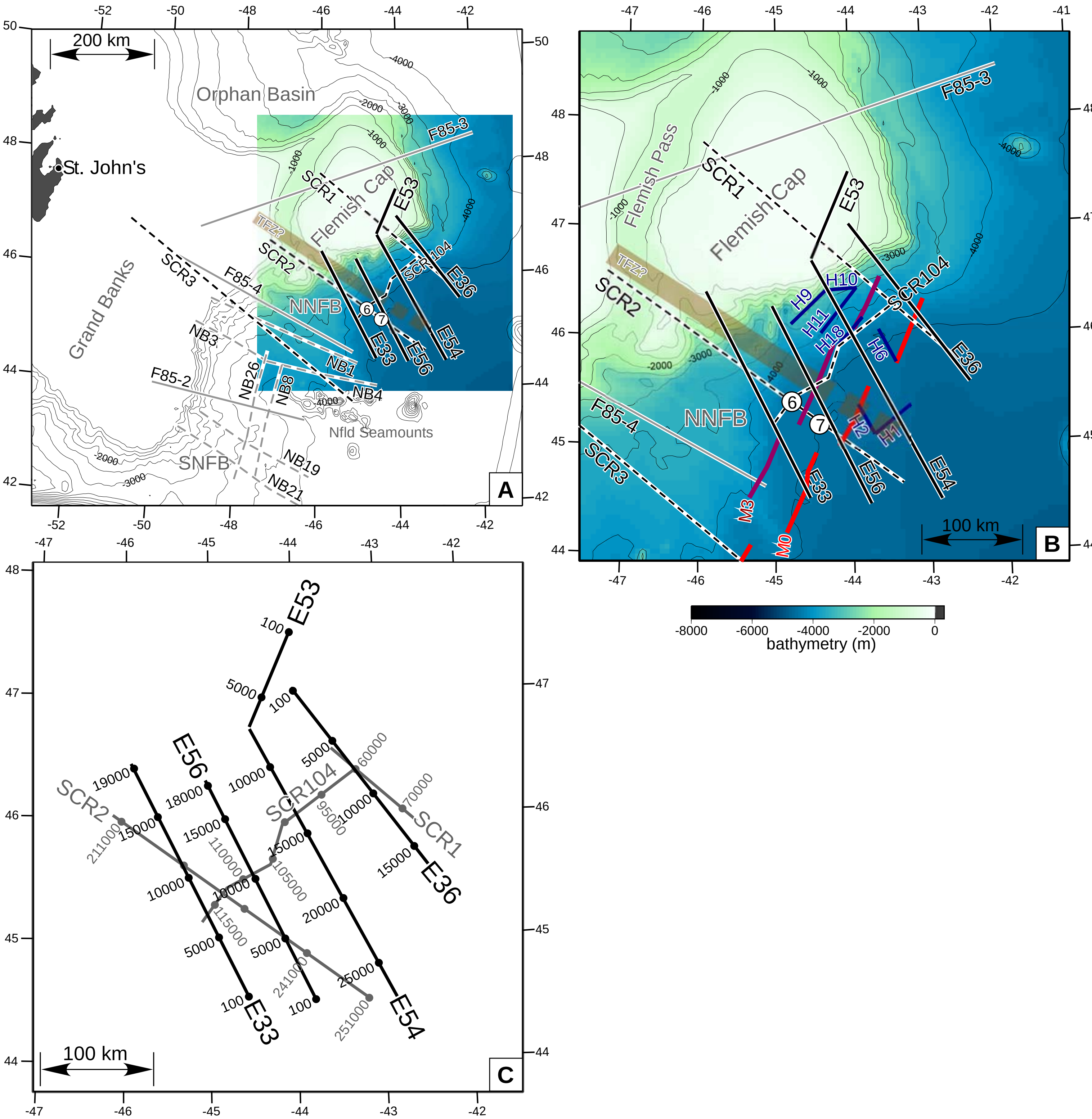
A
B
C
200 km
100 km
Orphan Basin
St. John's
Grand Banks
Flemish Cap
Flemish Pass
NNFB
SNFB
Nfld Seamounts
TFZ?
F85-3
F85-4
F85-2
SCR1
SCR2
SCR3
SCR104
E53
E36
E56
E33
E54
NB1
NB3
NB4
NB8
NB19
NB21
NB26
H1
H2
H6
H9
H10
H11
H18
M0
M3
bathymetry (m)

Figure 2

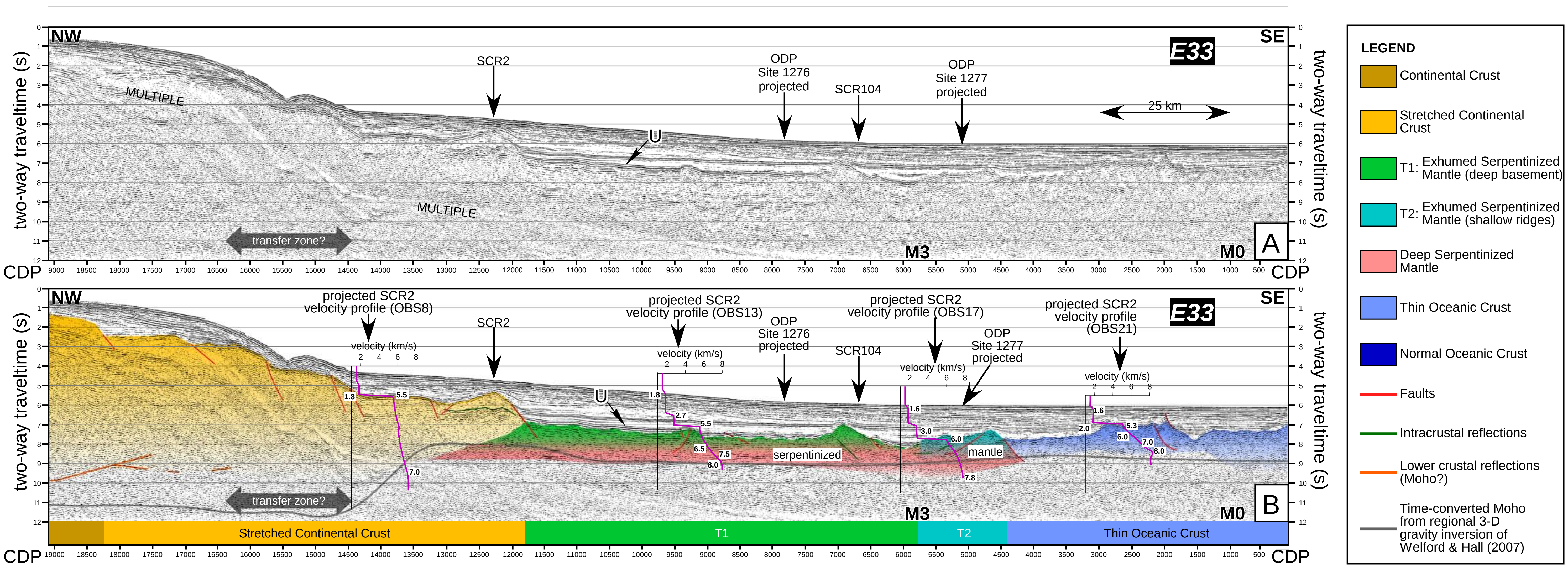
NW
SE
E33
two-way traveltime (s)
MULTIPLE
SCR2
ODP
Site 1276
projected
SCR104
ODP
Site 1277
projected
25 km
U
transfer zone?
M3
M0
A
CDP
projected SCR2
velocity profile (OBS8)
projected SCR2
velocity profile (OBS13)
projected SCR2
velocity profile (OBS17)
projected SCR2
velocity profile
(OBS21)
velocity (km/s)
serpentinized
mantle
B
Stretched Continental Crust
T1
T2
Thin Oceanic Crust
LEGEND
Continental Crust
Stretched Continental Crust
T1: Exhumed Serpentinized Mantle (deep basement)
T2: Exhumed Serpentinized Mantle (shallow ridges)
Deep Serpentinized Mantle
Thin Oceanic Crust
Normal Oceanic Crust
Faults
Intracrustal reflections
Lower crustal reflections (Moho?)
Time-converted Moho from regional 3-D gravity inversion of Welford & Hall (2007)

Figure 3

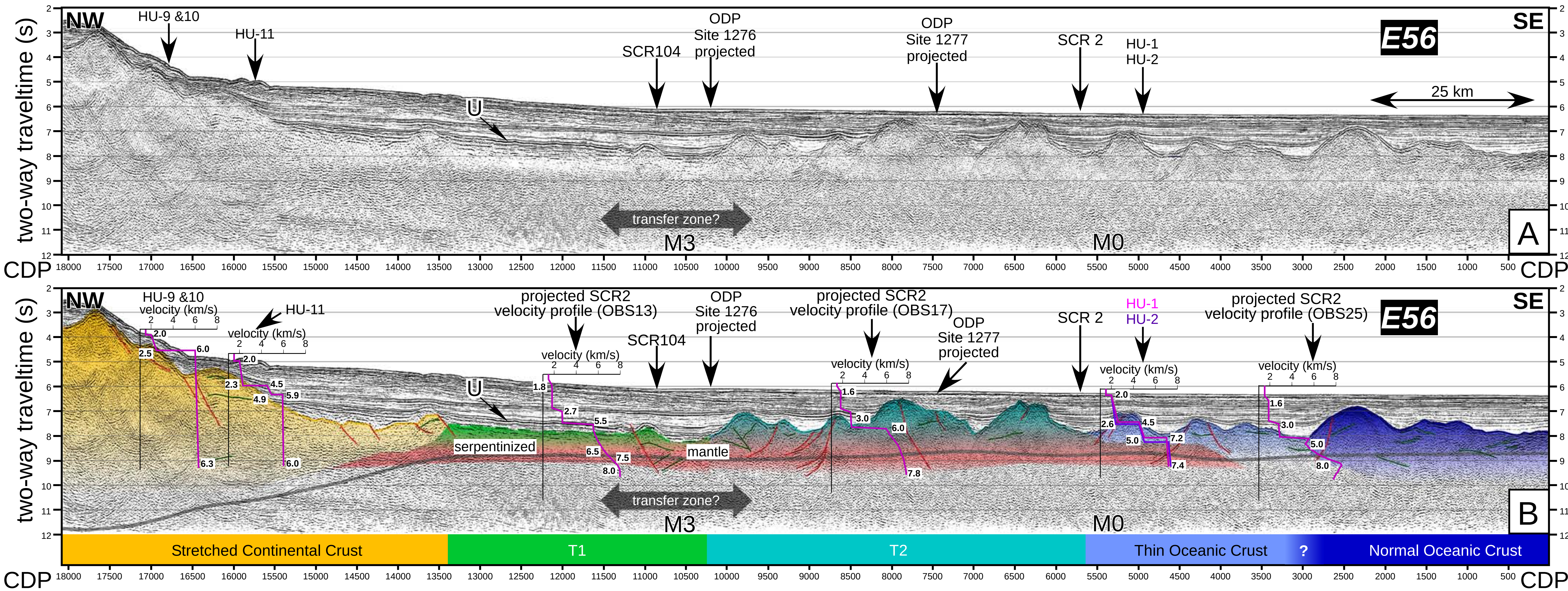
NW
SE
E56
HU-9 &10
HU-11
SCR104
ODP Site 1276 projected
ODP Site 1277 projected
SCR 2
HU-1
HU-2
25 km
U
transfer zone?
M3
M0
A
B
two-way traveltime (s)
CDP
projected SCR2 velocity profile (OBS13)
projected SCR2 velocity profile (OBS17)
projected SCR2 velocity profile (OBS25)
velocity (km/s)
serpentinized
mantle
Stretched Continental Crust
T1
T2
Thin Oceanic Crust
?
Normal Oceanic Crust

Figure 4

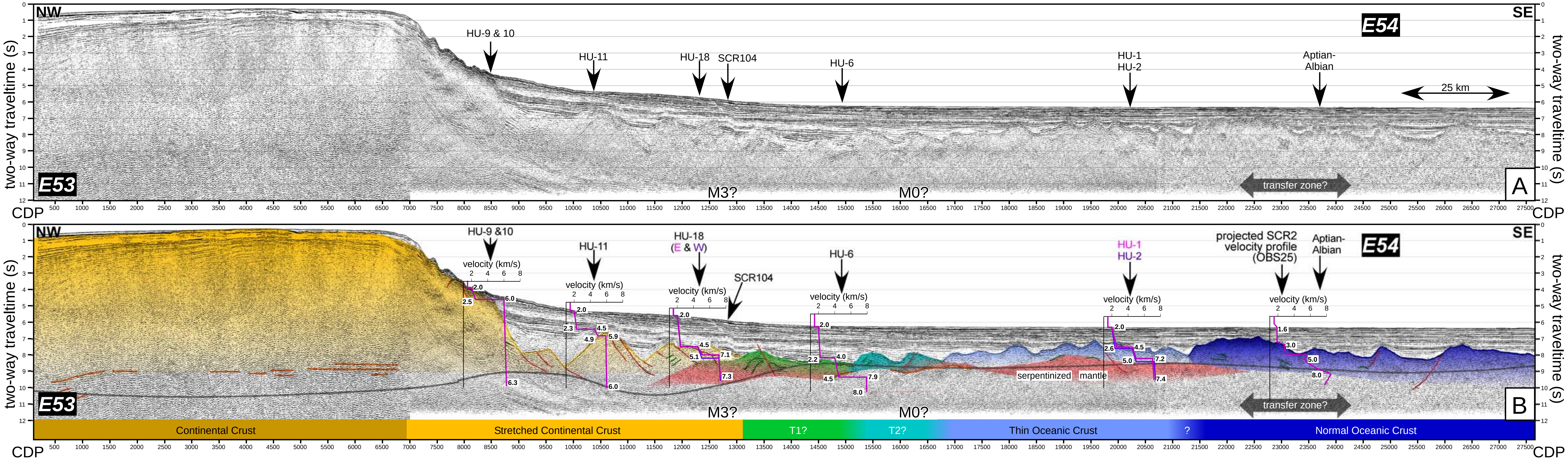
NW
SE
E54
E53
HU-9 & 10
HU-11
HU-18
SCR104
HU-6
HU-1
HU-2
Aptian-
Albian
25 km
transfer zone?
M3?
M0?
A
B
two-way traveltime (s)
CDP
HU-9 &10
HU-18
(E & W)
projected SCR2
velocity profile
(OBS25)
velocity (km/s)
serpentinized mantle
Continental Crust
Stretched Continental Crust
T1?
T2?
Thin Oceanic Crust
?
Normal Oceanic Crust

Figure 5

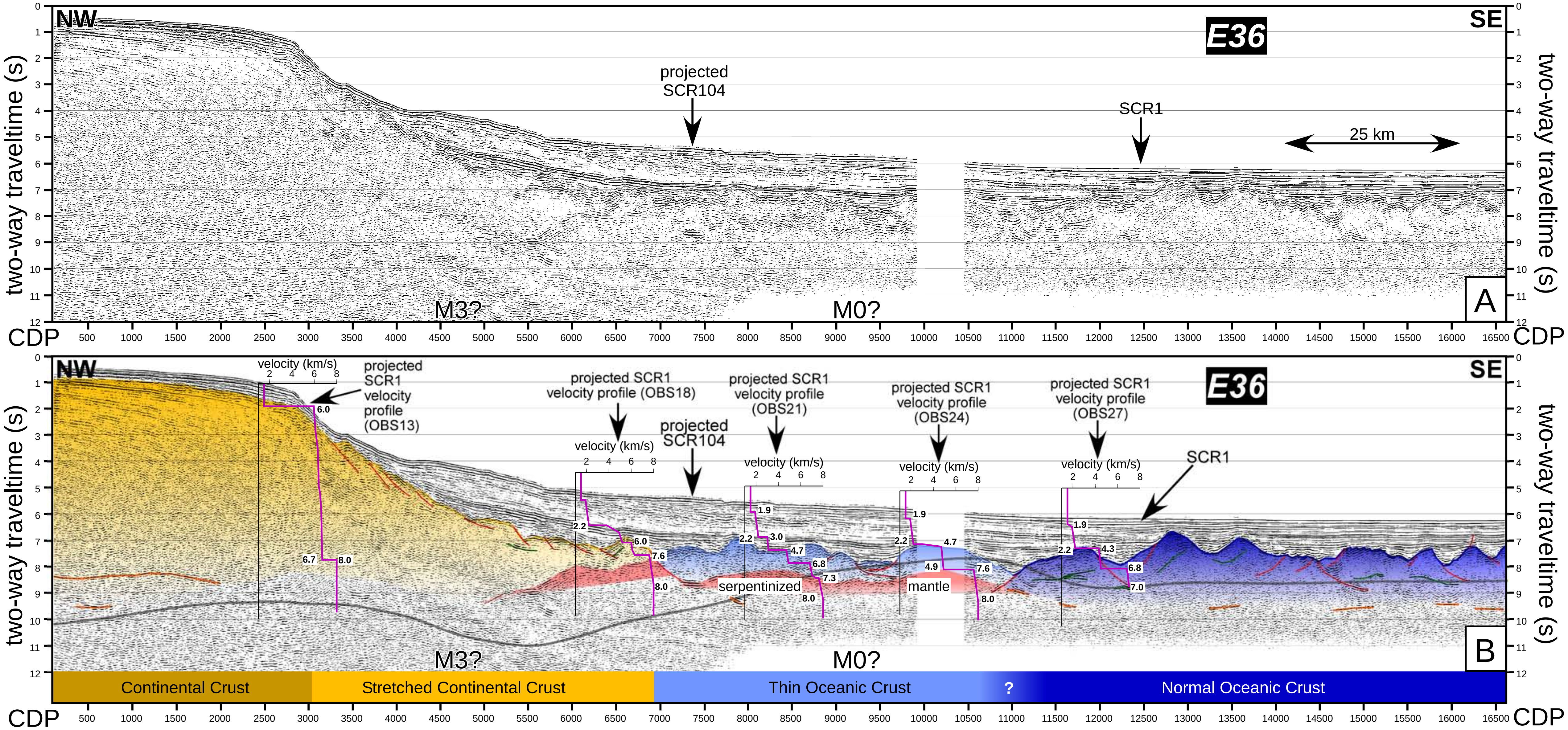

NW
SE
E36
projected SCR104
SCR1
25 km
M3?
M0?
A
two-way traveltime (s)
CDP
velocity (km/s)
projected SCR1 velocity profile (OBS13)
projected SCR1 velocity profile (OBS18)
projected SCR1 velocity profile (OBS21)
projected SCR1 velocity profile (OBS24)
projected SCR1 velocity profile (OBS27)
serpentinized
mantle
B
Continental Crust
Stretched Continental Crust
Thin Oceanic Crust
?
Normal Oceanic Crust

Figure 6

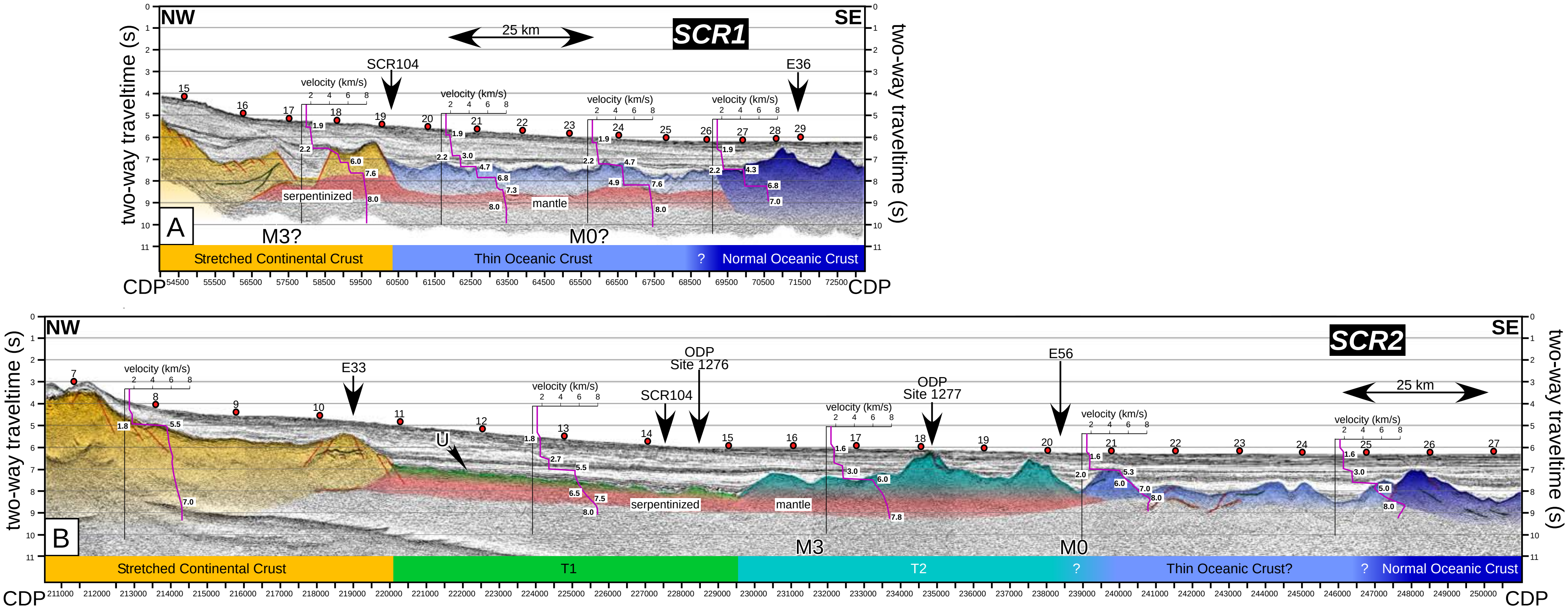

NW
SE
SCR1
25 km
SCR104
E36
velocity (km/s)
two-way traveltime (s)
serpentinized
mantle
M3?
M0?
A
Stretched Continental Crust
Thin Oceanic Crust
Normal Oceanic Crust
CDP
SCR2
E33
ODP Site 1276
ODP Site 1277
E56
U
M3
M0
B
T1
T2
Thin Oceanic Crust?

Figure 7

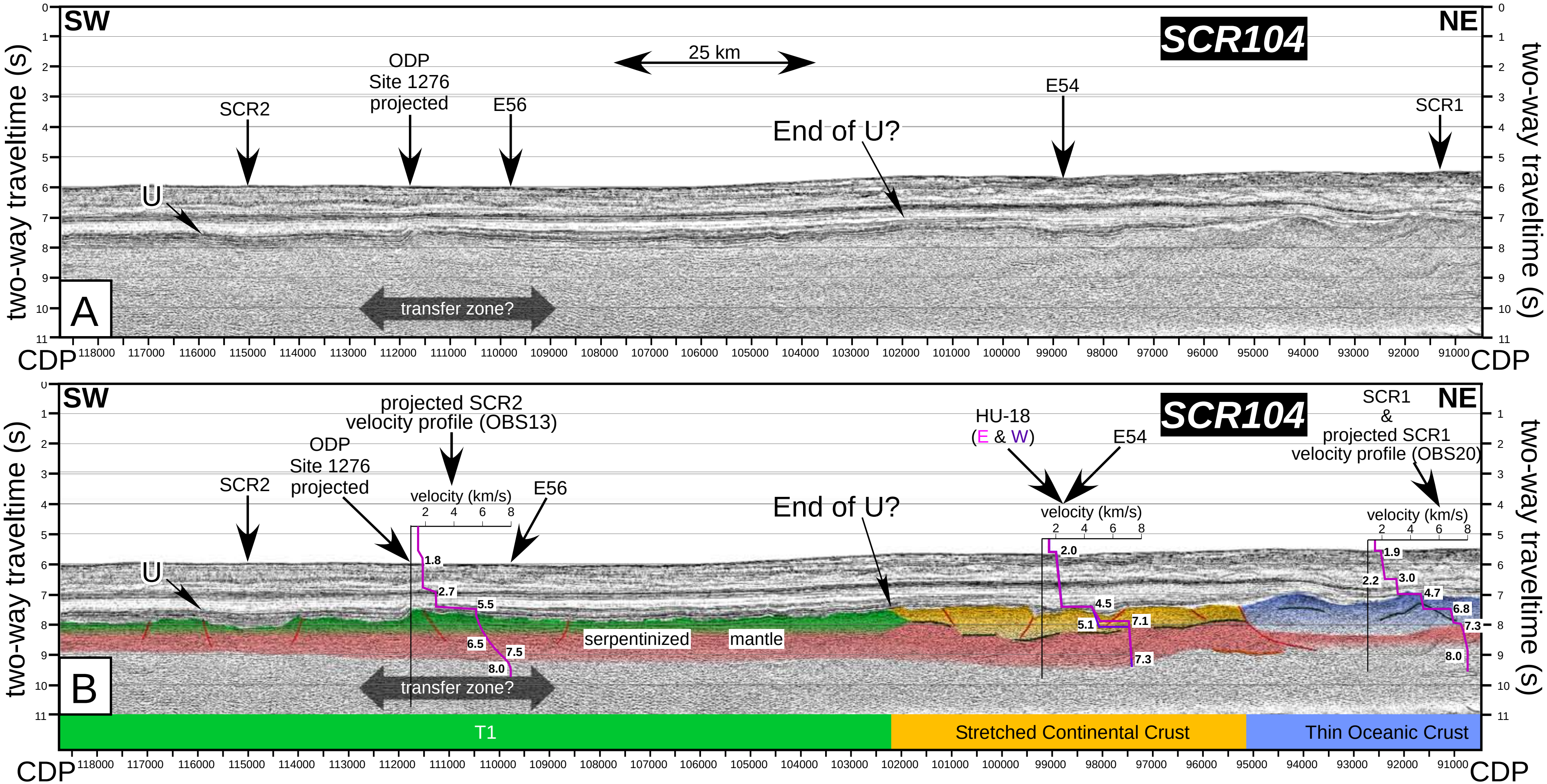

SW
NE
SCR104
25 km
ODP
Site 1276
projected
SCR2
E56
E54
SCR1
End of U?
U
transfer zone?
A
two-way traveltime (s)
CDP
SW
NE
SCR104
projected SCR2
velocity profile (OBS13)
ODP
Site 1276
projected
SCR2
E56
velocity (km/s)
HU-18
(E & W)
E54
SCR1
&
projected SCR1
velocity profile (OBS20)
End of U?
serpentinized
mantle
transfer zone?
B
T1
Stretched Continental Crust
Thin Oceanic Crust
two-way traveltime (s)
CDP

Figure 8

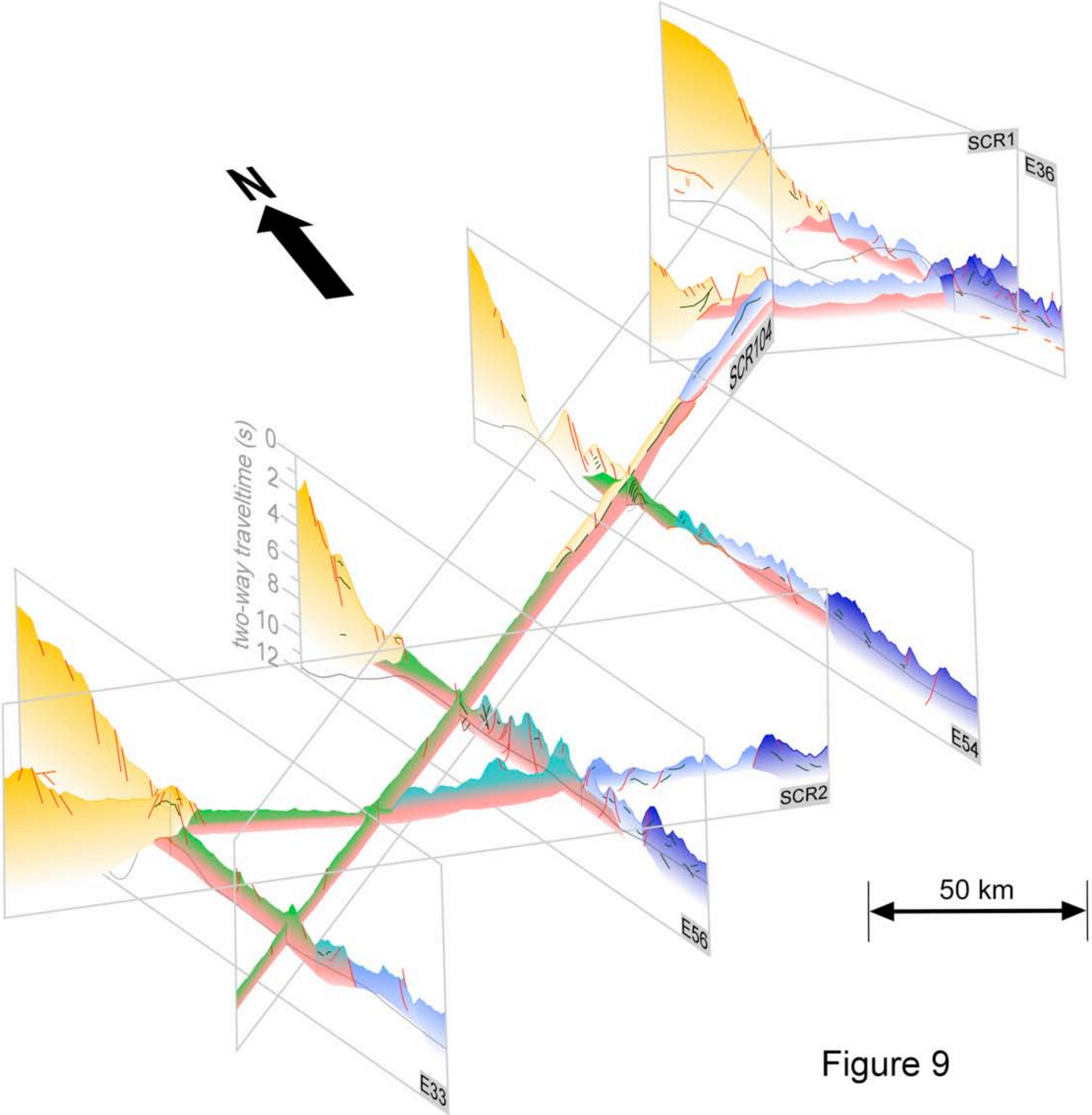
N
two-way traveltime (s)
0
2
4
6
8
10
12
SCR1
E36
SCR104
E54
SCR2
E56
E33
50 km

Figure 9

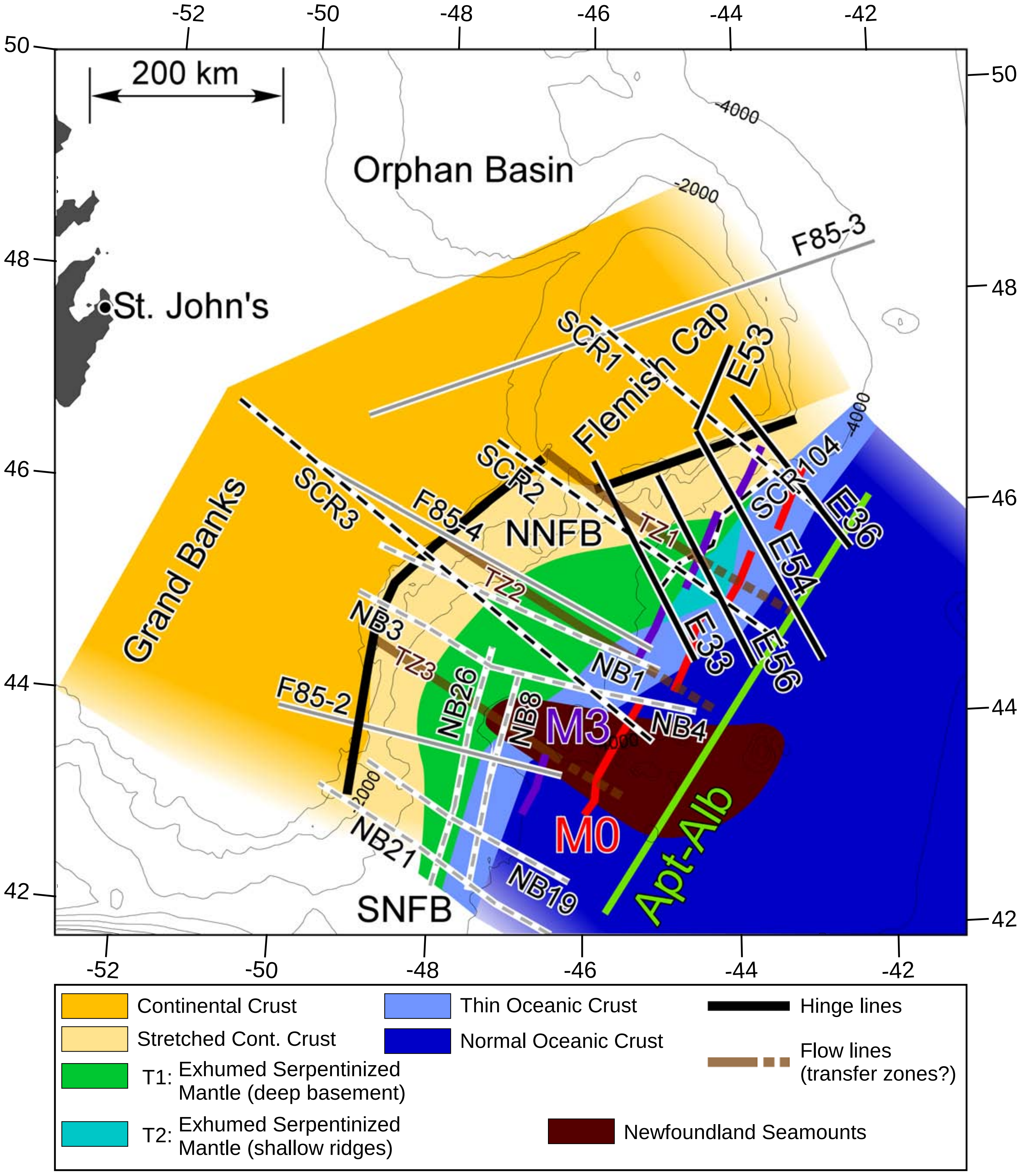

200 km
Orphan Basin
St. John's
Grand Banks
Flemish Cap
NNFB
SNFB
F85-3
F85-4
F85-2
SCR1
SCR2
SCR3
SCR104
E53
E36
E54
E33
E56
NB1
NB3
NB4
NB8
NB19
NB21
NB26
TZ1
TZ2
TZ3
M3
M0
Apt-Alb
-4000
-2000
Continental Crust
Stretched Cont. Crust
T1: Exhumed Serpentinized Mantle (deep basement)
T2: Exhumed Serpentinized Mantle (shallow ridges)
Thin Oceanic Crust
Normal Oceanic Crust
Hinge lines
Flow lines (transfer zones?)
Newfoundland Seamounts

Figure 10

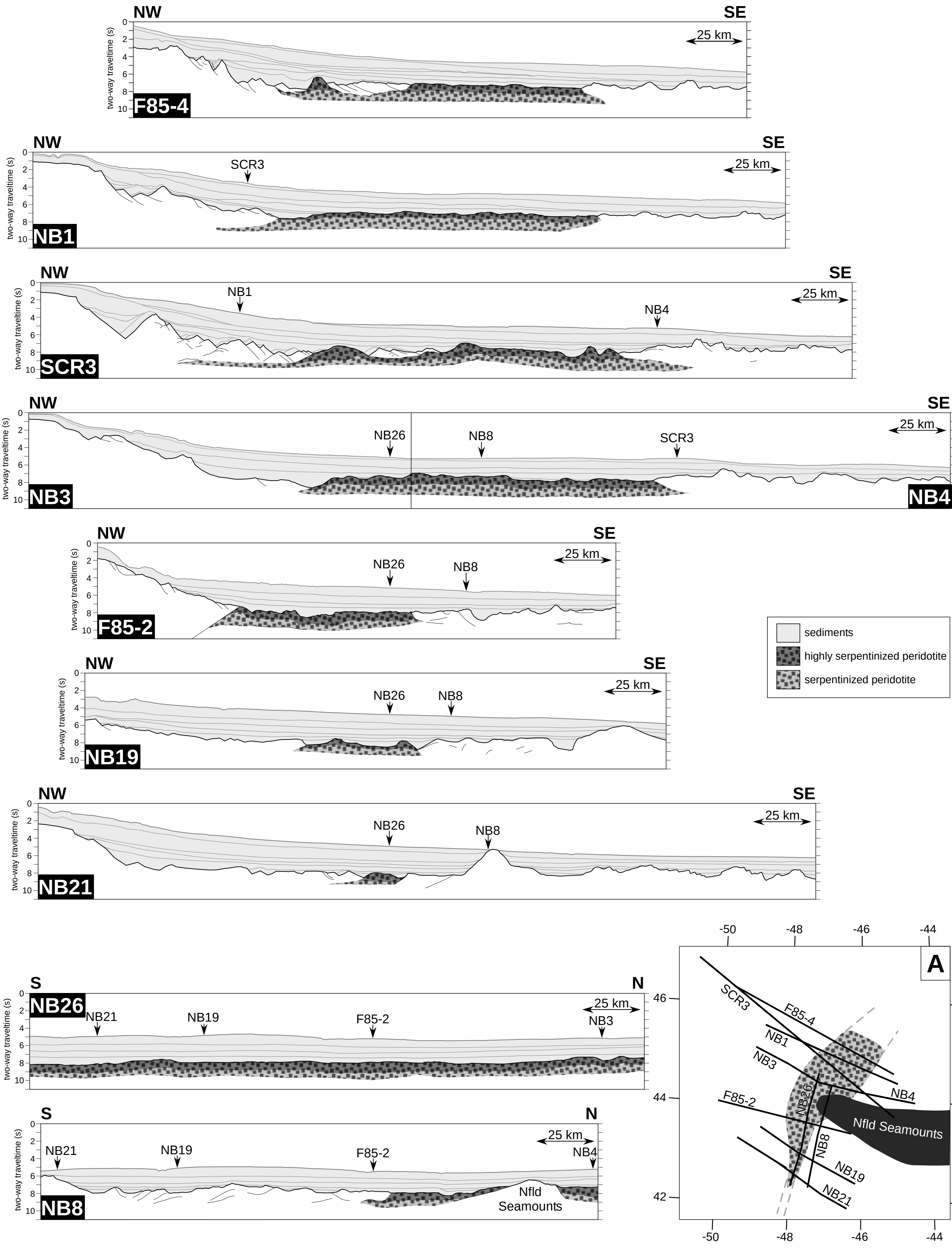

NW
SE
25 km
two-way traveltime (s)
F85-4
NB1
SCR3
NB1
NB4
NB3
NB26
NB8
SCR3
NB4
F85-2
NB19
NB21
sediments
highly serpentinized peridotite
serpentinized peridotite
S
N
NB26
NB21
NB19
F85-2
NB3
NB8
Nfld
Seamounts
A
Nfld Seamounts

Figure 11

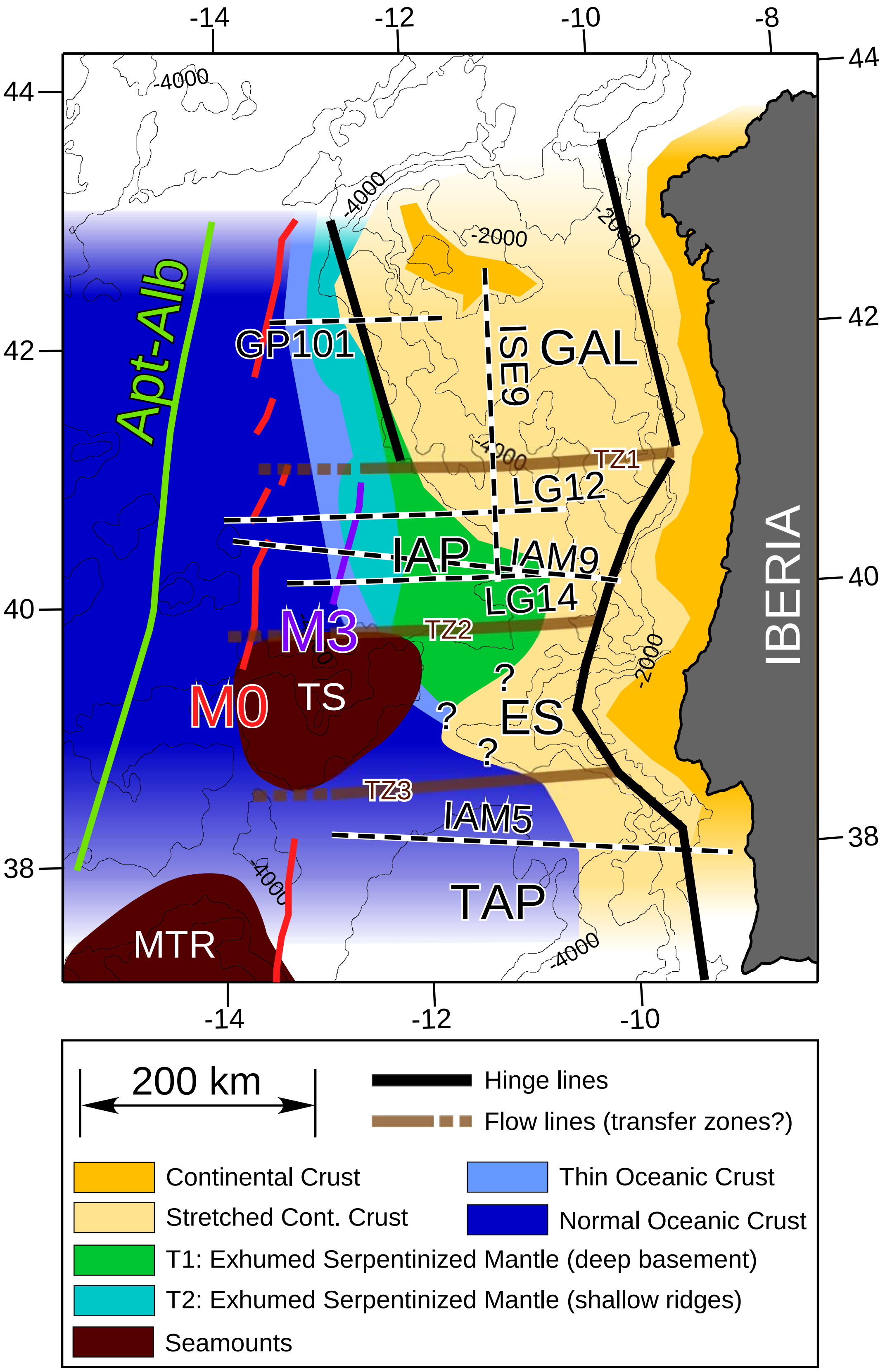

-14
-12
-10
-8
44
42
40
38
-4000
-2000
-2000
-2000
-4000
-4000
Apt-Alb
GP101
ISE9
GAL
TZ1
LG12
IAP
IAM9
LG14
M3
TZ2
M0
TS
ES
TZ3
IAM5
TAP
MTR
IBERIA
200 km
Hinge lines
Flow lines (transfer zones?)
Continental Crust
Thin Oceanic Crust
Stretched Cont. Crust
Normal Oceanic Crust
T1: Exhumed Serpentinized Mantle (deep basement)
T2: Exhumed Serpentinized Mantle (shallow ridges)
Seamounts

Figure 12

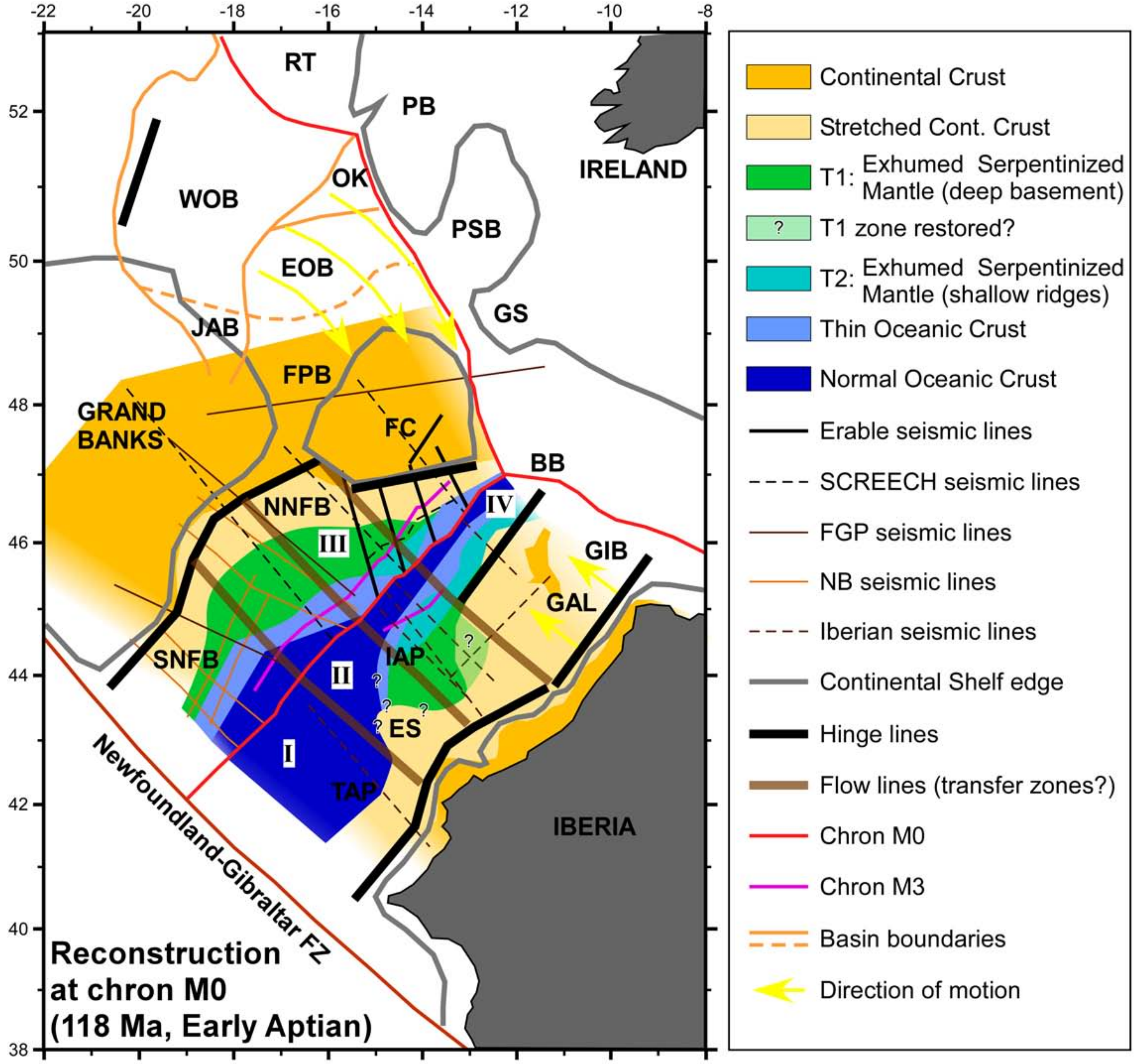

RT
PB
WOB
OK
IRELAND
PSB
EOB
GS
JAB
FPB
GRAND BANKS
FC
BB
NNFB
IV
III
GIB
GAL
SNFB
IAP
II
ES
I
TAP
IBERIA
Newfoundland-Gibraltar FZ
Reconstruction at chron M0 (118 Ma, Early Aptian)
Continental Crust
Stretched Cont. Crust
T1: Exhumed Serpentinized Mantle (deep basement)
T1 zone restored?
T2: Exhumed Serpentinized Mantle (shallow ridges)
Thin Oceanic Crust
Normal Oceanic Crust
Erable seismic lines
SCREECH seismic lines
FGP seismic lines
NB seismic lines
Iberian seismic lines
Continental Shelf edge
Hinge lines
Flow lines (transfer zones?)
Chron M0
Chron M3
Basin boundaries
Direction of motion

Figure 13

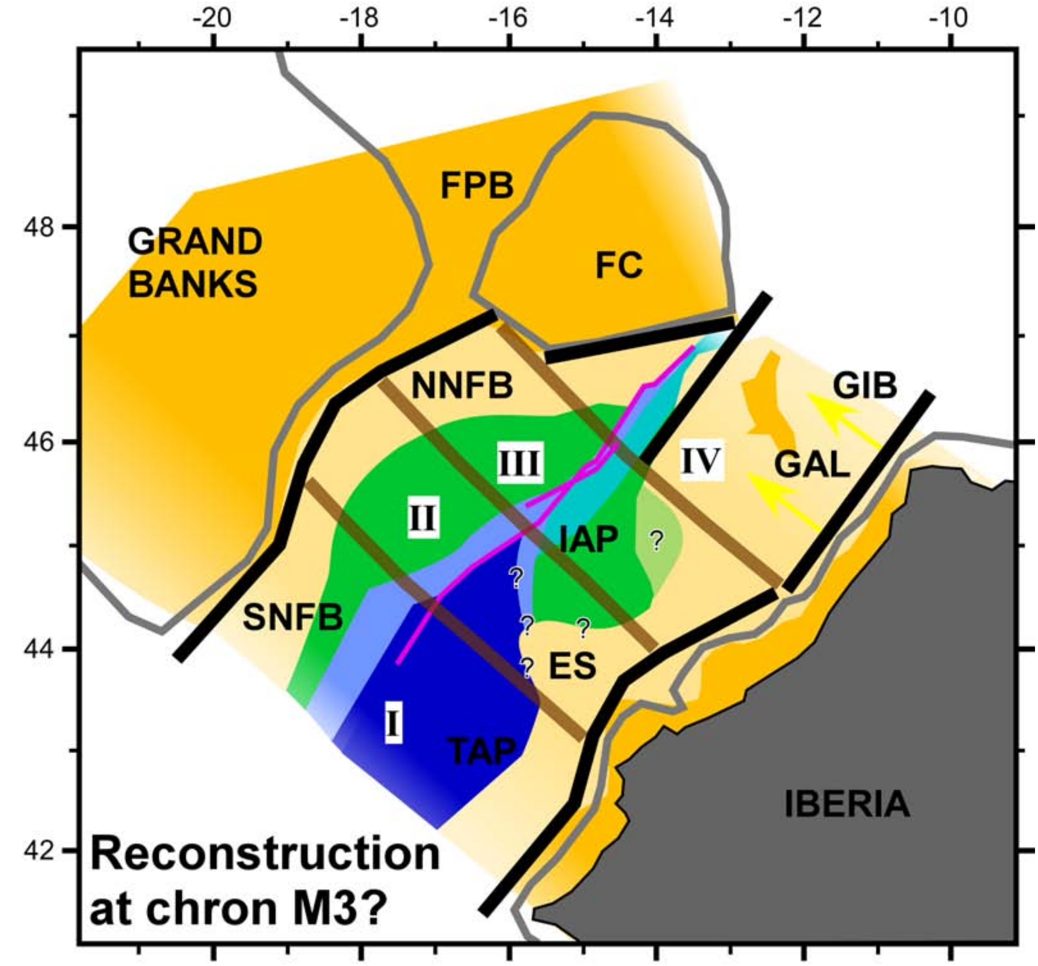
-20
-18
-16
-14
-12
-10
48
46
44
42
FPB
GRAND
BANKS
FC
NNFB
GIB
III
IV
GAL
II
IAP
?
SNFB
ES
I
TAP
IBERIA
Reconstruction
at chron M3?

Figure 14

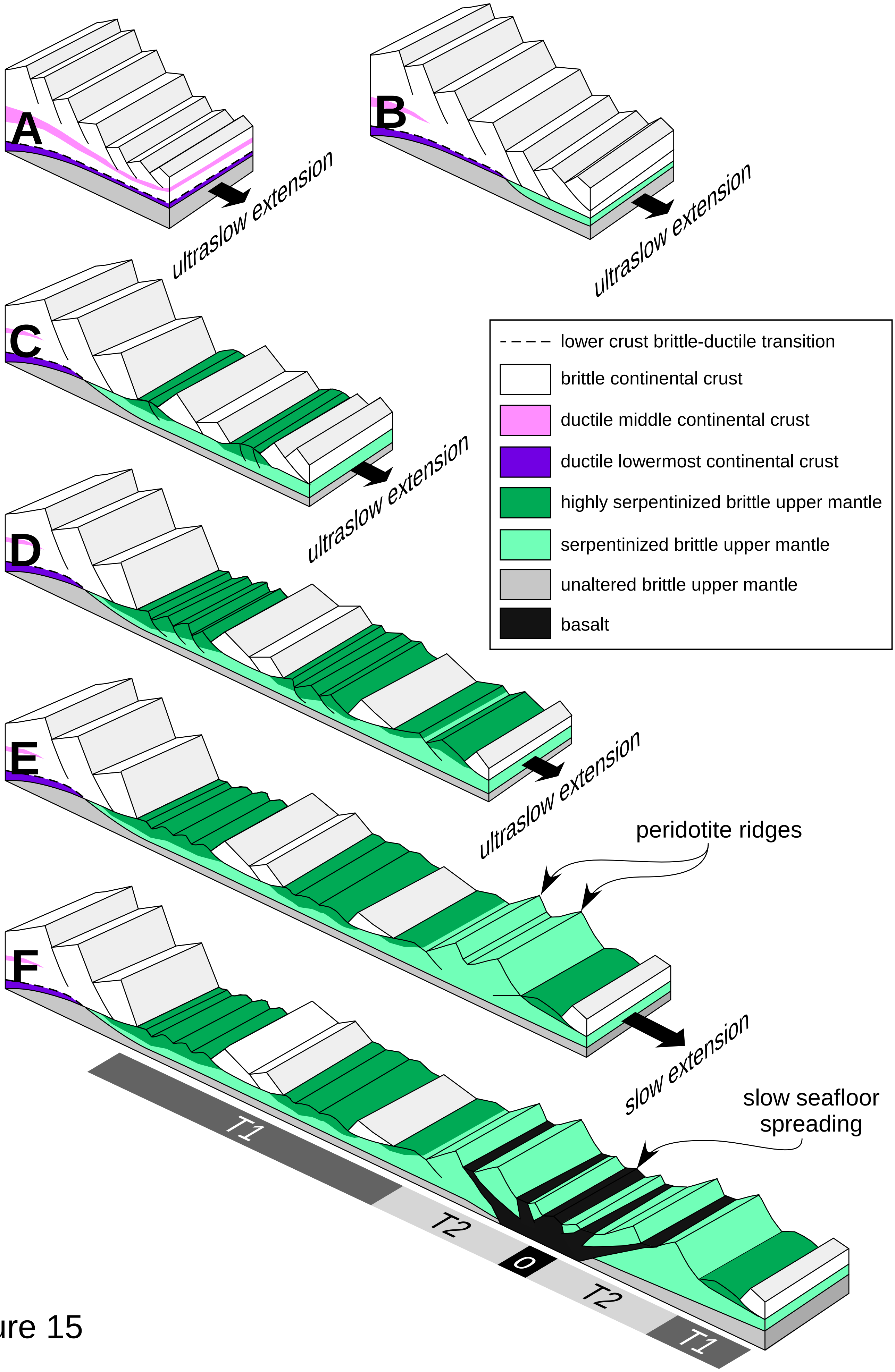
A
B
C
D
E
F
ultraslow extension
ultraslow extension
ultraslow extension
ultraslow extension
slow extension
lower crust brittle-ductile transition
brittle continental crust
ductile middle continental crust
ductile lowermost continental crust
highly serpentinized brittle upper mantle
serpentinized brittle upper mantle
unaltered brittle upper mantle
basalt
peridotite ridges
slow seafloor spreading
T1
T2
0
T2
T1

Figure 15